ESR SPIN PROBE AND SPIN LABELLED STUDIES OF CARDIOLIPIN

BY

LOUIE FOON YIP

B.Sc. University of British Columbia, 1977

A THESIS SUBMITTED IN PARTIAL FULFILLMENT OF
THE REQUIREMENTS FOR THE DEGREE OF
MASTER OF SCIENCE
IN
THE FACULTY OF GRADUATE STUDIES
(Department of Chemistry)

We accept this thesis as conforming
to the required standard

THE UNIVERSITY OF BRITISH COLUMBIA

JULY, 1981

In presenting this thesis in partial fulfilment of the requirements for an advanced degree at the University of British Columbia, I agree that the Library shall make it freely available for reference and study. I further agree that permission for extensive copying of this thesis for scholarly purposes may be granted by the head of my department or by his or her representatives. It is understood that copying or publication of this thesis for financial gain shall not be allowed without my written permission.

Department of CHEMISTRY

The University of British Columbia
2075 Wesbrook Place
Vancouver, Canada
V6T 1W5

Date AUG 18 1981

ABSTRACT

The phospholipid, diphosphatidylglycerol (cardiolipin) forms liquid-crystalline phases having lamellar and hexagonal structures depending on the amount of water, the temperature and the presence of cations. ESR studies of cardiolipin in the lamellar and the hexagonal phases using the 5-doxyl stearic acid spin probe were repeated to resolve a discrepency in the results reported in the literature. The spin probe was further used to follow the lamellar to hexagonal phase transition of cardiolipin as the Ca^{2+} concentration is increased from 0.0 to 50 mole % of Ca^{2+}.

Cardiolipin has been spin labelled at the polar head group by reaction with (2,2,5,5-tetramethylpyrroline-1-oxyl-3-carboxyl)-p-toluenesulfonate. The spin labelled cardiolipin (SLCL) was characterized using TLC and ESR. The SLCL was used in the ESR study of cardiolipin in the various phases.

The results from this work indicate with the use of spin probes and spin labels, it is possible to distinquish the different phases of cardiolipin. Furthermore the results suggest that non-bilayer structures exist between 9 to 29 mole % of Ca^{2+}. The data can be interpreted in terms of a temperature induced lateral phase separation of inverted micelles.

ABSTRACT

The phospholipid, diphosphatidylglycerol (cardiolipin) forms liquid-crystalline phases having lamellar and hexagonal structures depending on the amount of water, the temperature and the presence of cations. ESR studies of cardiolipin in the lamellar and the hexagonal phases using the 5-doxyl stearic acid spin probe were repeated to resolve a discrepency in the results reported in the literature. The spin probe was further used to follow the lamellar to hexagonal phase transition of cardiolipin as the Ca^{2+} concentration is increased from 0.0 to 50 mole % of Ca^{2+}.

Cardiolipin has been spin labelled at the polar head group by reaction with (2,2,5,5-tetramethylpyrroline-1-oxyl-3-carboxyl)-p-toluenesulfonate. The spin labelled cardiolipin (SLCL) was characterized using TLC and ESR. The SLCL was used in the ESR study of cardiolipin in the various phases.

The results from this work indicate with the use of spin probes and spin labels, it is possible to distinquish the different phases of cardiolipin. Furthermore the results suggest that non-bilayer structures exist between 9 to 29 mole % of Ca^{2+}. The data can be interpreted in terms of a temperature induced lateral phase separation of inverted micelles.

TABLE OF CONTENTS

LIST OF TABLES

LIST OF FIGURES

ACKNOWLEDGEMENT

First, I wish to express my sincere gratitude to my supervisor, Dr. F. G. Herring, for his continual guidance and encouragement throughout the course of this work.

I wish to thank Dr. A. Storr for the loan of his laboratory equipment. I am also grateful to Paul Phillips for his help and interest in my work.

CHAPTER 1

INTRODUCTION

The phospholipid, diphosphatidylglycerol (cardiolipin) was first isolated from beef heart and partially purified by Mary C. Pangborn [1]. Pangborn demonstrated that cardiolipin was identical to the active lipid antigen in the serodiagnosis of syphilis previously found by Wassermann et al [2,3]. Cardiolipin with lecithin and cholesterol in a properly balanced mixture (about 1:9:60 by molar ratio) exhibits a specific complement-fixing activity with sera from syphilitic patients resembling the activity of beef heart extracts prepared for diagnostic use [4]. This spurred further work on the purification and structure determination of cardiolipin.

Cardiolipin (CL) is found in many different types of tissues: mammalian tissues, fish and avian muscles, plant leaves and algae, invertebrates and protozoa, yeast and bacteria [5,6]. In mammalian tissues cardiolipin is found mainly with unsaturated fatty acid acyl chains, constituting 2-10% of total phospholipid. Cardiolipin from bacteria contains mostly saturated fatty acid acyl chains and those from plants have various amounts of saturated and unsaturated fatty acids. In human organs, cardiolipin is found to the greatest extent in heart and skeletal muscles. In general cardiolipin is characteristically associated with subcellular membraneous particles displaying high metabolic activity, especially the mitochondria of animal tissues, plants and yeast.

The structure of cardiolipin has been the subject of many investigations. The one originally proposed by Pangborn for cardiolipin from beef heart is in figure 1.1 [7]. This structure with one oleic and five linoleic acid residues agreed with the available analytical data. The glycerol/phosporus/fatty acid ratio is 4:3:6. The suggested structure contained a backbone of GPGPGPG (G=glycerol, P=phosporic acid) in which the six hydroxyl groups are acylated. With more improved purification procedures of cardiolipin the glcerol/phosphorus/fatty acid ratio was founded to be 3:2:4 with varying fatty acyl chains. The proposed general structure for cardiolipin is shown in figure 1.2 [5,8]. The structure for beef heart cardiolipin is a GPGPG backbone with variable R1, R2, R3, and R4. The same GPGPG skeleton was found for cardiolipin from plants.

Cardiolipin from different sources exhibits variability in the fatty acyl chains attached to the common glycerol and phosphate grouping. For example, the fatty acid compostion of cardiolipin from beef heart is found to be mainly oleic acid and linoleic acid, 12% and 80% respectively. The study of different organs of various mammals showed that, typically, cardiolipin in mammalian tissues is unsaturated. The acyl chains found are composed of 60-80% linoleic acid and 10-20% oleic acid. For whole tissues of plant origin, the fatty acid had a composition range of: palmitic acid 10-34% stearic 1-14%, oleic 5-15%, linoleic 20-60% and linolenic from 0-57%.

Many research studies have been performed in an attempt to correlate the existence of cardiolipin with a functional role either in mitochondrial or prokaryotic membranes. No conclusions

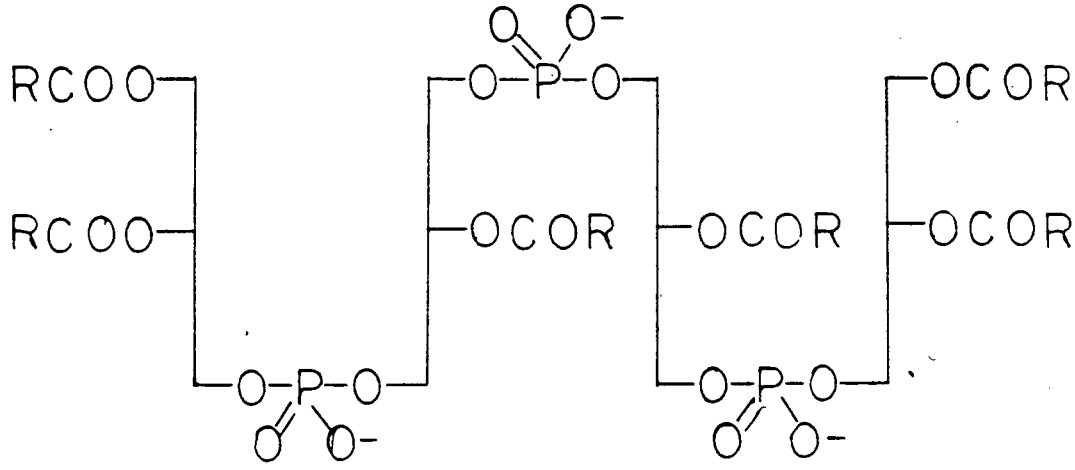

Figure 1.1 Original structure of cardiolipin proposed by Pangborn.

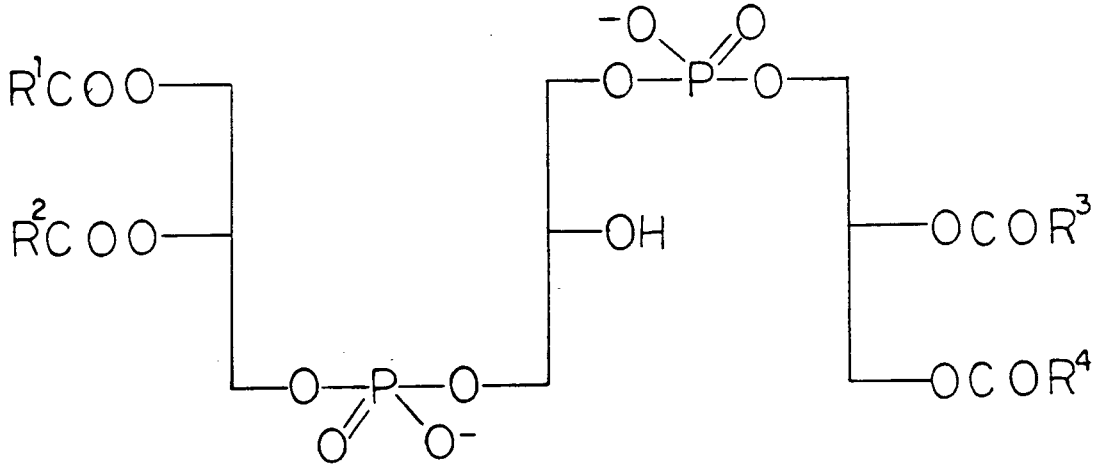

Figure 1.2 General structure of cardiolipin.

have yet been reached, but many suggestions have been extrapolated from model or in vitro experiments [5,8,9].

The question that provided the impetus for this work is the role of cardiolipin in erythrocyte acetylcholinesterase [9]. The lipoprotein erythrocyte acetylcholinesterase catalyzes acetylcholine hydrolysis on the outer surface of the cell membrane. Acetylcholinesterase from bovine erythrocytes gave a non-linear Arrhenius plot (log of its activity vs 1/T). The break in the Arrhenius plot disappeared and the activity decreased when the lipoprotein was treated with high salt and Ca^{2+}-chelating reagents. The lipid cardiolipin was lost from acetylcholinesterease during this procedure. Addition of cardiolipin to the enyzme in the presence of calcium chloride restored the break in the Arrhenius plot and its activity. The structure of the cardiolipin species in the lipoprotein complex is unknown, and it was felt that a spin label study may help in elucidating this.

Phospholipids in the presence of water in their hydrated state aggregate to form large multimolecular structures. In these structures they may form polymorphic phases such as micellar, bilayer or hexagonal configurations [10]. It has been postulated that the preference of a lipid species for a given structure reflects the dynamic molecular shape assumed by the individual phospolipid components as illustrated in figure 1.3 [11]. Lysophospholipids and detergents form a micellar phase due to their inverted cone-shape such that the polar head group is larger then the tail section. Lipids such as phosphatidylcholine and phosphatidylglycerol assume a cylindrical shape which form

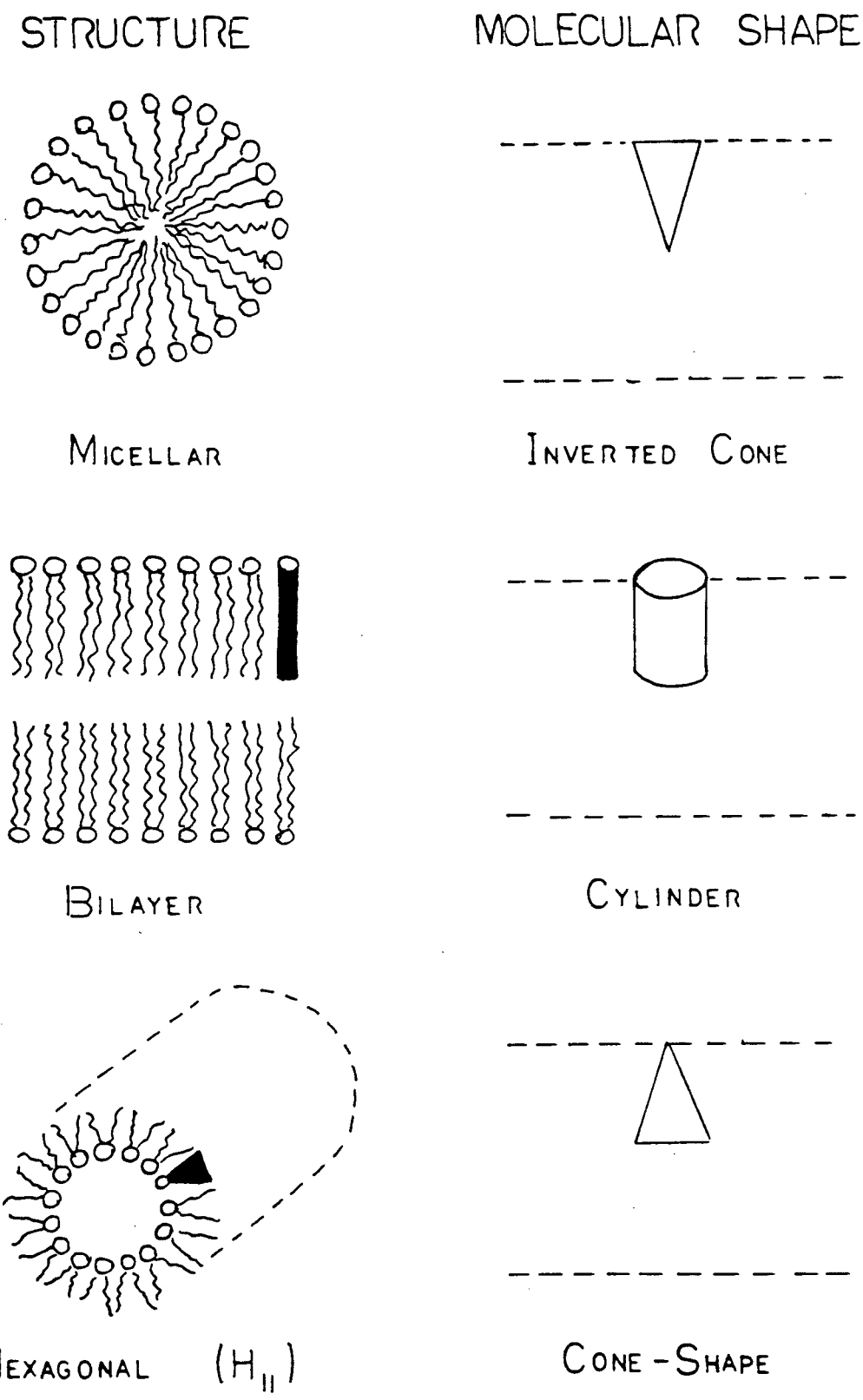

Figure 1.3 Lipid structure and corresponding molecular shape.

the bilayer phase. Cardiolipin as the mono-valent cation salt form also prefers the bilayer structure. Phosphatidylethanolamine (unsaturated), phosphatidic acid-Ca^{2+} and cardiolipin-Ca^{2+} which are approximately cone-shaped form the hexagonal phase. These lipids possess a headgroup region smaller than the tail and are best suited for the hexagonal phase.

Cardiolipin can exist as a lamellar or hexagonal structure depending on temperature, water content and the presence of cations. The disodium salt of cardiolipin will form liquid crystalline phases having lamellar and hexagonal structure depending on the amount of water present. Cardiolipin will also precipitate as the salt of divalent cations to give the hexagonal structure. Rand and Sengupta [11] using X-ray diffraction techniques have shown that cardiolipin in the lamellar phase will precipitate to form the hexagonal phase with calcium. Magnesium and Barium divalent cations will also induce the hexagonal phase, but not at all temperatures and concentrations. Freeze-fracture and freeze-etching techniques can also be employed with electron micrographs to demonstrate the difference between the two phases [12]. Another method for determining the phase of cardiolipin is by employing ^{31}P NMR techniques. Cullis et al [10,13] have demonstrated with ^{31}P NMR that there is a difference in the NMR signal from cardiolipin in the lamellar and the NMR signal from the hexagonal phases.

ESR studies employing spin probes have also been performed in order to study the structural organization of cardiolipin in aqueous dispersions. The results from these two studies are

contradictory. The work of Hegner et al [14] showed differences in the ESR spectra of a spin probe incorporated in the lamellar and hexagonal phases, whereas the Hsia paper [15] shows no difference between the two. In this work we have repeated and extended the ESR study using the spin probe 5-doxyl-stearic acid in the hope of sorting out this discrepency. The results of this additional investigation also provide valuable information as to the formation of the hexagonal phase.

An alternative to spin probe studies in the various phases of cardiolipin, is to spin label the cardiolipin itself. There are two possible places to spin label the cardiolipin, the polar head group (secondary-OH) or the hydrocarbon chain. Two groups have reported methods for spin labelling at both these positions [16,17].

The structures of cardiolipin in the two phases, shown in figure 1.4, suggest that spin labelling the head group will be preferable. From X-ray data, the polar to polar transbilayer distance are 34.5-37.1 Å, and 35.6-41.4 Å for the lamellar and hexagonal phases respectively [11]. Thus the change in the hydrocarbon chain region between the two phases appears to be small. Whereas if the headgroup is spin labelled, the spin label in the polar head region would go from almost unrestricted motion in the lamellar structure to the very restricted motion in the hexagonal structure. In the hexagonal phase the water channels have diameters of 14.2-16.6 Å, as shown in figure 1.4, and as a consequence dramatic changes in the ESR spectra of labelled cardiolipin can be expected.

As indicated, it appears to be desirable to spin label the

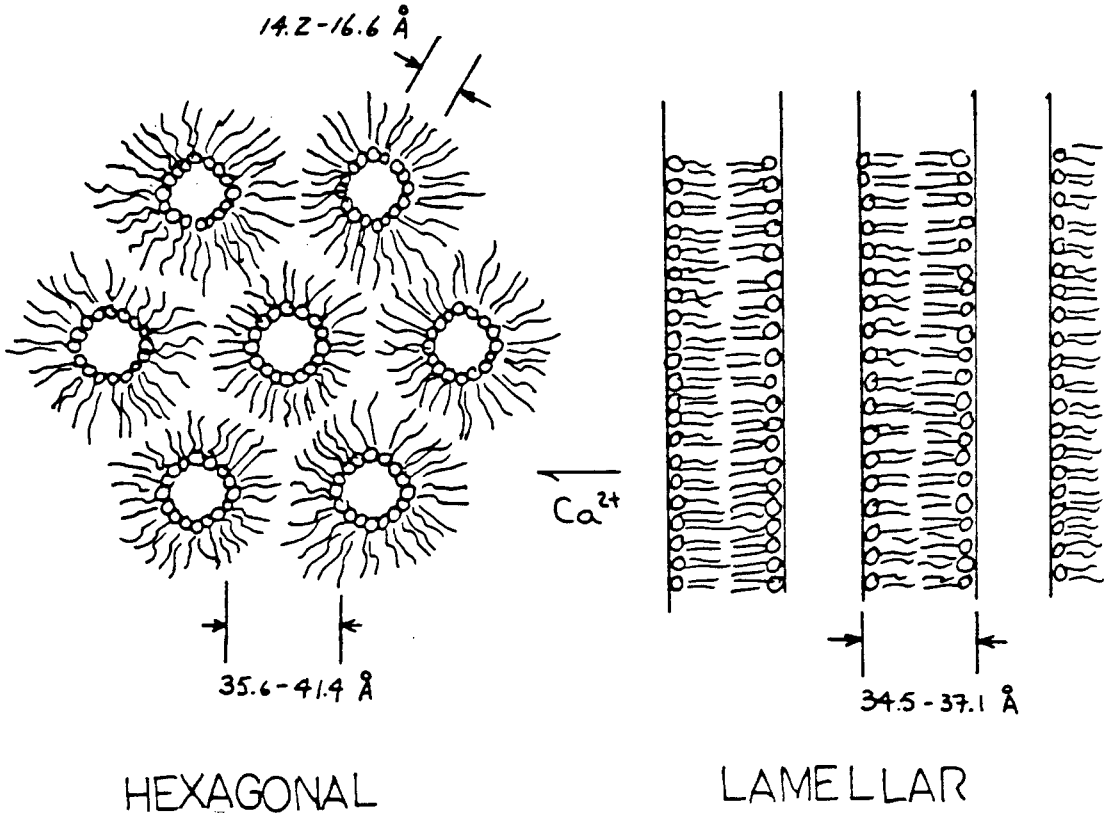

Figure 1.4 Hexagonal and lamellar phases of cardiolipin with structural dimensions.

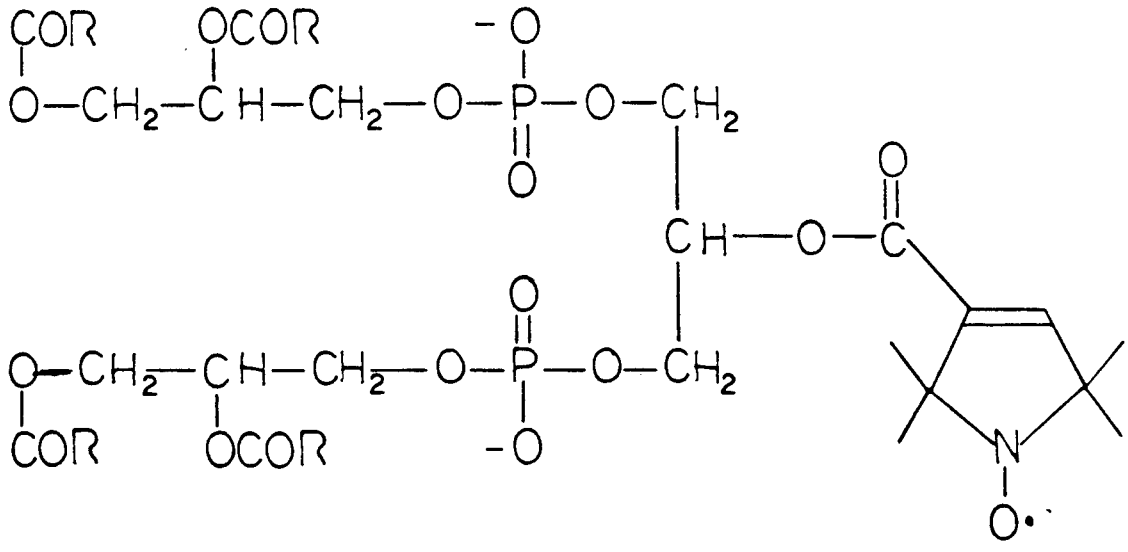

Figure 1.5 General structure of spin labelled cardiolipin.

polar head group of cardiolipin. Many groups have attempted the acetylation of the hydroxyl group of cardiolipin with varying degrees of success [5]. Attempts such as using acetic anhydride (radioactive) in benzene/pyridine yield 5-10% acetylation at 90°C for 10 minute or at 20°C for 12 hour [5]. Alternatively reacting cardiolipin with excess myristoyl chloride in anhydrous chloroform at 20°C for 48 hour underwent about 5% conversion [5]. This shows the reactivity of the hydroxyl group is low. Longer reaction times resulted in extensive decomposition of the starting material into lyso-derivatives of cardiolipin.

Landriscina et al have spin labelled the free hydroxyl group of cardiolipin using 2,2,5,5-tetramethypyrroline-n-oxide-3-carboxyl chloride [17]. The reaction was performed in anhydrous chloroform containing pyridine at 60°C for 12-14 hour. This method was used in the begining of the current study to prepare the spin labelled cardiolipin (SLCL) as illustrated in figure 1.5. But the prolonged heating at high temperatures used in this method resulted in the formation of lysocardiolipin. A more gentle method has been developed in this work using a modification of Keana's [18] acylating procedure.

The objective of this work is to use the spin probe 5-doxyl stearic acid to investigate the formation of the hexagonal phase and to clarify the previously obtained ambiguous results using this probe. In addition these studies will be supplemented by studying the ESR spectra of spin labelled cardiolipin in both the lamellar and hexagonal phases.

CHAPTER 2

THEORY

2.1 Electron Spin Resonance of Nitroxide Radicals.

The theory of Electron Spin Resonance (ESR) spectroscopy has been presented in detail in a number of texts and articles (19-23), so only the salient features will be presented here. ESR spectroscopy is a sensitive technique for the detection of species with unpaired electrons in the system under study. The application of ESR in biological systems such as membrane studies which often do not contain paramagnetic centres have been achieved by the introduction of molecules containing an unpaired electron. Nitroxide spin labels and spin probes are widely used for this purpose [19,23]. The term nitroxide spin probe refers to any system containing a nitroxide moiety not covalently attached to the system and when the nitroxide is covalently attached to a molecule of interest it is then refered to as a nitroxide spin label. The nitroxide spin moiety is shown in figure 2.1 which possess an unpaired electron localized mainly in a $2P_z$ orbital on the nitrogen atom.

2.2 ESR Spectra of Nitroxides.

a) Solution

For a nitroxide radical in solution in which the electron spin interacts via hyperfine coupling with the nitrogen nucleus of nuclear spin quantum number I, the magnetic Hamiltonian is

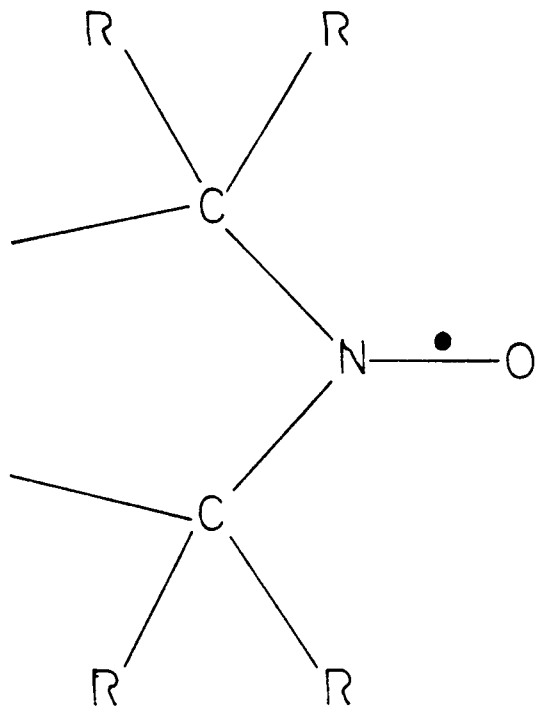

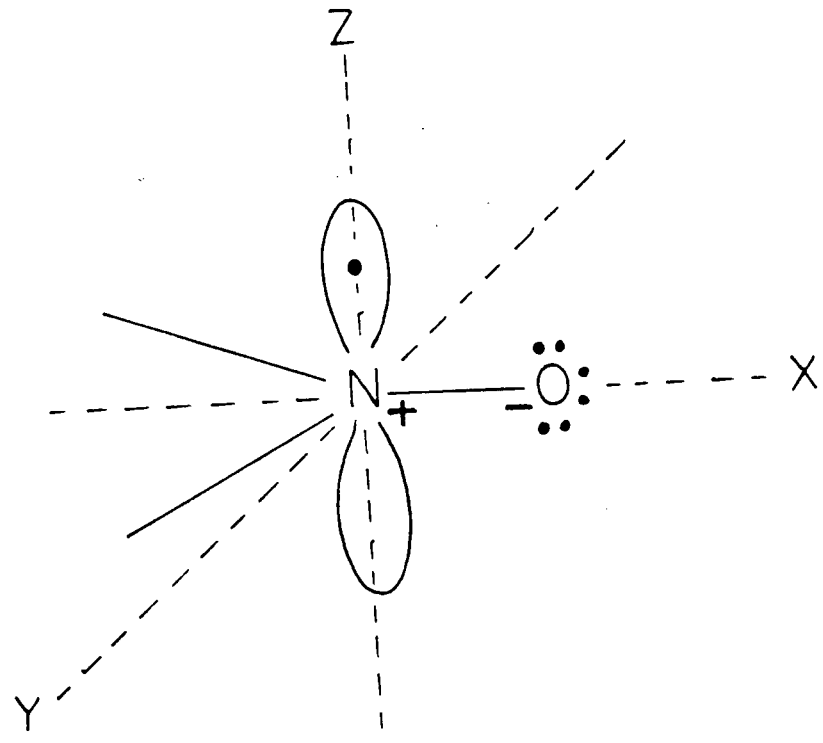

Figure 2.1 Nitroxide spin moiety.

given by

$$\hat{H} = g_o \beta_e \underset{\sim}{H_o} \bullet \underset{\sim}{\hat{S}} + a_o \underset{\sim}{\hat{S}} \bullet \underset{\sim}{\hat{I}} \qquad (2.1)$$

g_o = the g factor, a constant characteristic of the electron in the radical in question

β_e = the Bohr magneton = $\frac{eh}{2M_e C}$

M_e = mass of electron

$\underset{\sim}{H_o}$ = is the applied magnetic field

$\underset{\sim}{\hat{S}}$ = electron spin operator

a_o = coupling constant

$\underset{\sim}{\hat{I}}$ = nuclear spin operator

The first order Hamiltionian is

$$\hat{H} = g_o \beta_e \hat{H}_o S_z + a_o \hat{S}_z \hat{I}_z \qquad (2.2)$$

The solution to the first order equation is

$$E_{(m_S, m_I)} = g_o \beta_e H_o m_S + a_o m_S m_I$$

m_S = eigen value of the electron spin angular momentum operator $\hat{S}_z$

m_I = eigen value of the nuclear spin angular momentum operator $\hat{I}_z$

All allowed ESR transitions usually satisfy the selection rules of $\Delta m_S = 1$, $\Delta m_I = 0$ for all nuclei. The energy difference of the levels involved in the allowed transition is

$$E_{(m_S)} = h\nu = E_{(m_S+1,m_I)} - E_{(m_S,m_I)} \qquad (2.3)$$
$$= g_o\beta_e H_o + a_o m_I$$

Thus for a nitroxide radical I=1, the spectrum will consists of three lines, corresponding to m =1, 0 and -1, with energies

$$\Delta E_{(m_I=1)} = g_o\beta_e H_o + a_o$$
$$\Delta E_{(m_I=0)} = g_o\beta_e H_o \qquad (2.4)$$
$$\Delta E_{(m_I=-1)} = g_o\beta_e H_o - a_o$$

respectively. The spectral lines are equally spaced and the separation between adjacent lines is a_o/h in frequency units. In ESR studies, the field is scanned at a fixed frequency ν, therefore the spacing becomes $a_o/g_o\beta_e$ in gauss.

b) Solid

A feature of ESR spectra is that the line positions and splittings between the lines depend on the direction of the magnetic field relative to the molecular axis or hyperfine axis. The directional dependence of the hyperfine and g-tensors are illustrated in figure 2.2. The figure shows the ESR spectra of a nitroxide free radicals oriented in a crystal lattice with the magnetic field paralled to each of the three principal directions. The spectral anisotropy can be specified by three g-values and three hyperfine constants. These are the principal values of the hyperfine and g-tensors:

T_{xx}, T_{yy}, T_{zz}

and

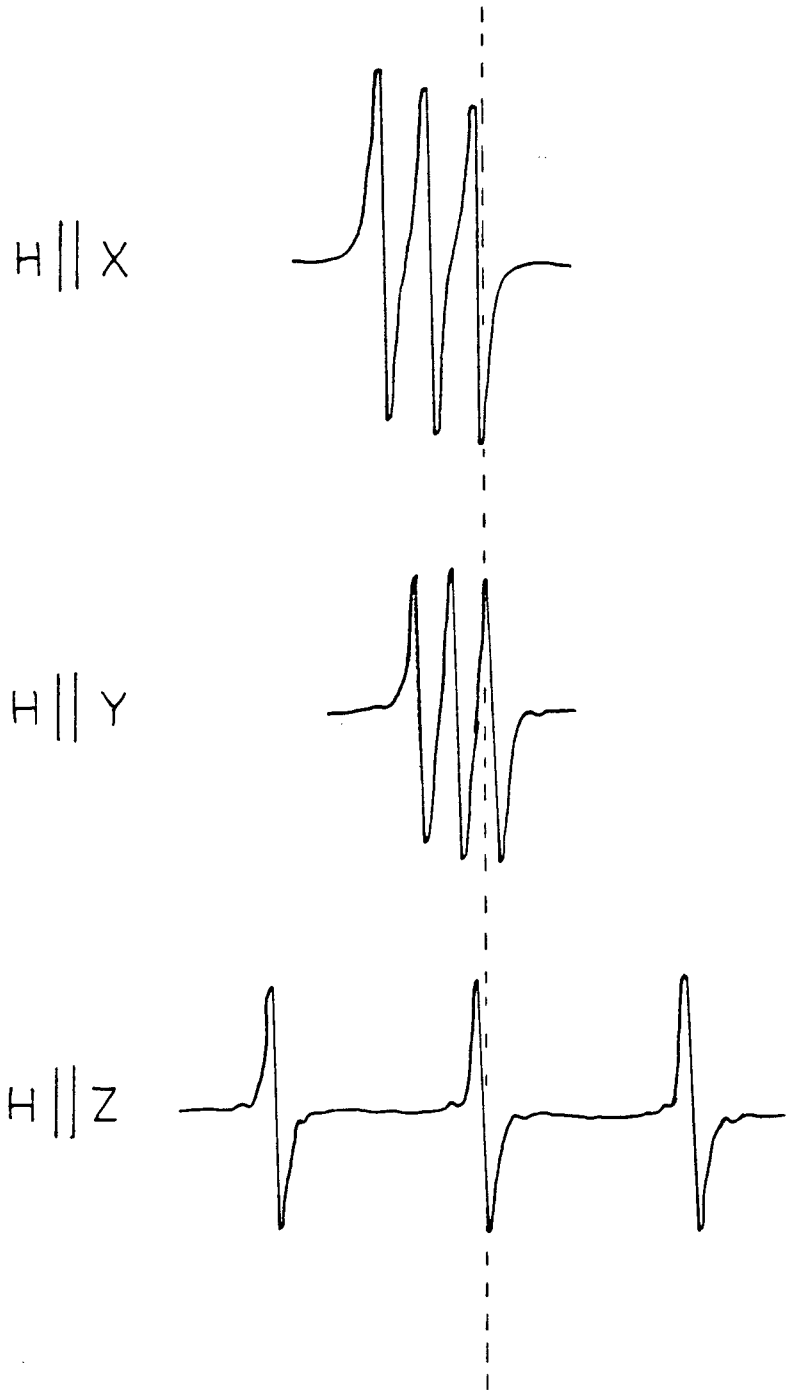

Figure 2.2 ESR spectra of spin probe in rigid matrix.

g_{xx}, g_{yy}, g_{zz}, respectively.

In many cases the molecular system is approximately axially symmetric and the principal values can then be expressed as:

$$T_{zz} = T_{\parallel}$$

$$T_{xx} = T_{yy} = T_{\perp}$$

$$g_{zz} = g_{\parallel}$$

$$g_{xx} = g_{yy} = g_{\perp}$$

The spectrum obtained from a solution of a nitroxide contains three sharp lines, but here the g and T anisotropies have been averaged out so that the line positions are determined by g_o and a_o, where

$$g_o = (g_{xx} + g_{yy} + g_{zz})/3$$

and (2.5)

$$a_o = (T_{xx} + T_{yy} + T_{zz})/3$$

To obtain the g tensor and hyperfine tensor components accurately a single crystal sample must be used to study the dependence of the nitroxide ESR spectrum on the angles between the applied magnetic field and the symmetry axis of the radical. This can also be done by doping a diamagnetic host crystal of known three dimensional structure with the nitroxide of interest. Usually single crystals and nitroxide doped host crystals are not available and the so-called polycrystalline powder spectrum is recorded (figure 2.3). In this case a computer simulation of the spectrum is required to obtain accurate values of T and g [19].

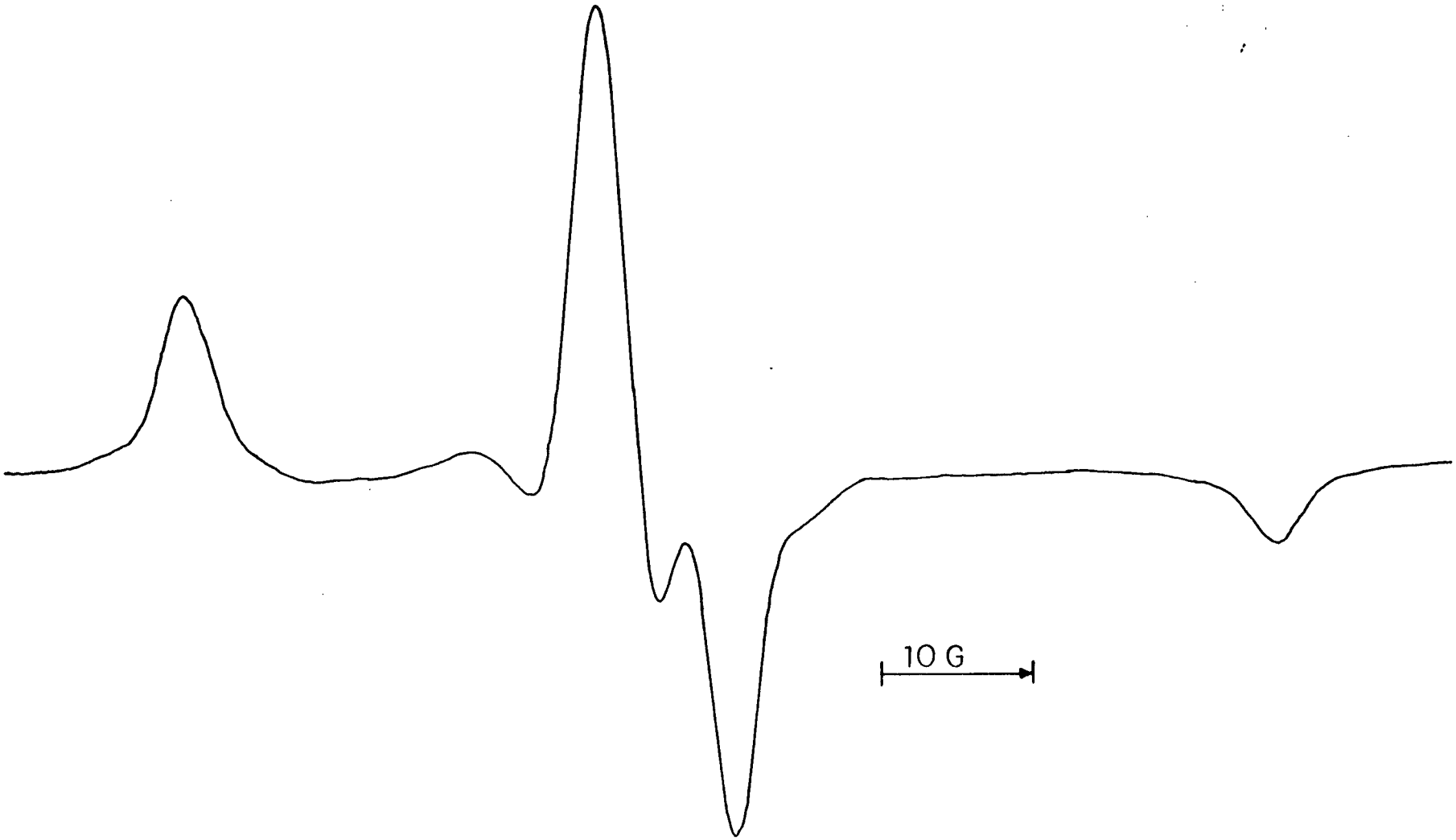

Figure 2.3 ESR spectrum of a polycrystalline solution of a nitroxide

2.3 Analysis of ESR Spectra.

A spin label ESR spectrum is extremely sensitive to the nature and the rate of the motion the spin label undergoes. If the motion is fast on the ESR time scale (correlation time τ_c < 10^{-9} s), the spectra will display g values and hyperfine splittings that are the averages of the principal components. The rate of the motion determines the relative widths of the various resonances. The narrow lines for rapid motion broaden as motion becomes slower. In the extreme case, when motion is very slow the spectra obtained are similiar to those from powders as illustrated in figure 2.3.

The analysis of spectral lineshape and linewidths has been performed in terms of a rotational correlation time for isotropic motion in the rapid tumbling limit [22]. The width ΔH_m of an individual line is given by:

$$\Delta H_m = A + Bm + Cm^2$$

where m is the z component of the nitrogen nuclear spin quantum number I=1, for ^{14}N, with the low field ,center and high field lines correspond to m = +1, 0, and -1 respectively. The terms B and C are functions of the peak-to-peak linewidth of the center line, ΔH_o and the amplitudes of the m-th lines, I_m. These two terms are related to the correlation time for isotropic motion according to the following equations [22] :

$$B = \Delta H_o \, (\sqrt{I_c/I_1} - \sqrt{I_o/I_{-1}})/2 \qquad (2.6)$$

$$= 0.103 \, \omega_e \{\Delta g \Delta a + 3(\delta g \delta a)\} \, \tau_B \{1 + 3(1 + \omega_e^2 \tau_B^2)^{-1}/4\}$$

$$C = \Delta H_o \left(\sqrt{I_o/I_1} + \sqrt{I_o/I_{-1}} - 2\right)/2 \qquad (2.7)$$

$$= 1.81X10^6 \{(\Delta a)^2 + 3(\delta a)^2\} \tau_c \{1 - 3(1 + \omega_N^2 \tau_c^2)^{-1}/8 - (1 + \omega_e^2 \tau_c^2)^{-1}/8\}$$

where

$$\Delta a = T_{zz} - (T_{xx} + T_{yy})/2$$

$$\Delta g = g_{zz} - (g_{xx} + g_{yy})/2$$

$$\delta a = (T_{xx} - T_{yy})/2$$

$$\delta g = (g_{xx} - g_{yy})/2$$

with the T terms in gauss, and $\omega_N = 8.8X10^6\ a_o$, where a_o is the isotropic hyperfine splitting, and ω_e is the ESR spectrometer frequency in angular units ($\omega = 2\pi\nu$). τ_B and τ_C are the correlation times calculated from B and C respectively. In order to calculate τ_B and τ_C the g tensor and hyperfine tensor have to be obtained from a spectrum of the nitroxide in a polycrystalline phase e.g. powder spectrum or low temperature glass spectrum.

In the region of rapid, isotropic motion the correlation times τ_B and τ_C should be equal. Recent work has indicated that the condition of isotropic motion rarely applies [22]. So most nitroxide molecules undergo anisotropic motion and the τ_B calculated is not equal to τ_C. The ratio of τ_C/τ_B indicates the preferential axis about which rotation takes place [25], thus for example $\tau_C/\tau_B > 1$, it is the y axis.

When the rotational motion is slow enough, as it is for 5-doxyl stearic acid spin probe in dispersions of lipids, such that the spectra approach the powder spectrum limit, the above analysis no longer applies. Another relatively simple method of analysis is possible. This is the method of measuring the order

parameter S. This requires the measurement of $2T'_{\parallel}$ and $2T'_{\perp}$ (twice the apparent hyperfine couplings of the nitroxide free radical). The order parameter S, assuming cylindrical symmetry along the long axis of the lipids is given by the following expression [19] :

$$S = (T'_{\parallel} - T'_{\perp})/\{ T_{zz} - (T_{xx} + T_{yy})/2 \} \qquad (2.8)$$

Alternatively, one can determine T_{zz} from an ESR spectrum of a polycrystalline solution of a nitroxide, then:

$$S = \frac{T'_{\parallel} - T'_{\perp}}{3(T - a')/2} \qquad (2.9)$$

$$a' = (T'_{\parallel} + 2T'_{\perp})/3$$

These equations hold for spin probes in which the nitroxide Z axis is parallel the long axis of the probe.

A common spin probe used in membrane research is the 5-doxyl-stearic acid probe shown in figure 2.4 whose nitroxide Z axis is parallel to the long axis. The long hydrophobic tail anchors the probe to the hydrophobic regions of a membrane system. The nitroxide moiety then monitors the environment of the bilayer around it. The ESR spectra of the probe can yield information concerning the structure of the lipids into which it is incorporated.

The measurement of $2T'_{\perp}$ is not possible at all temperatures, as is often the case for biological membranes, hence the evaluation of S is then difficult. An alternative approach is to

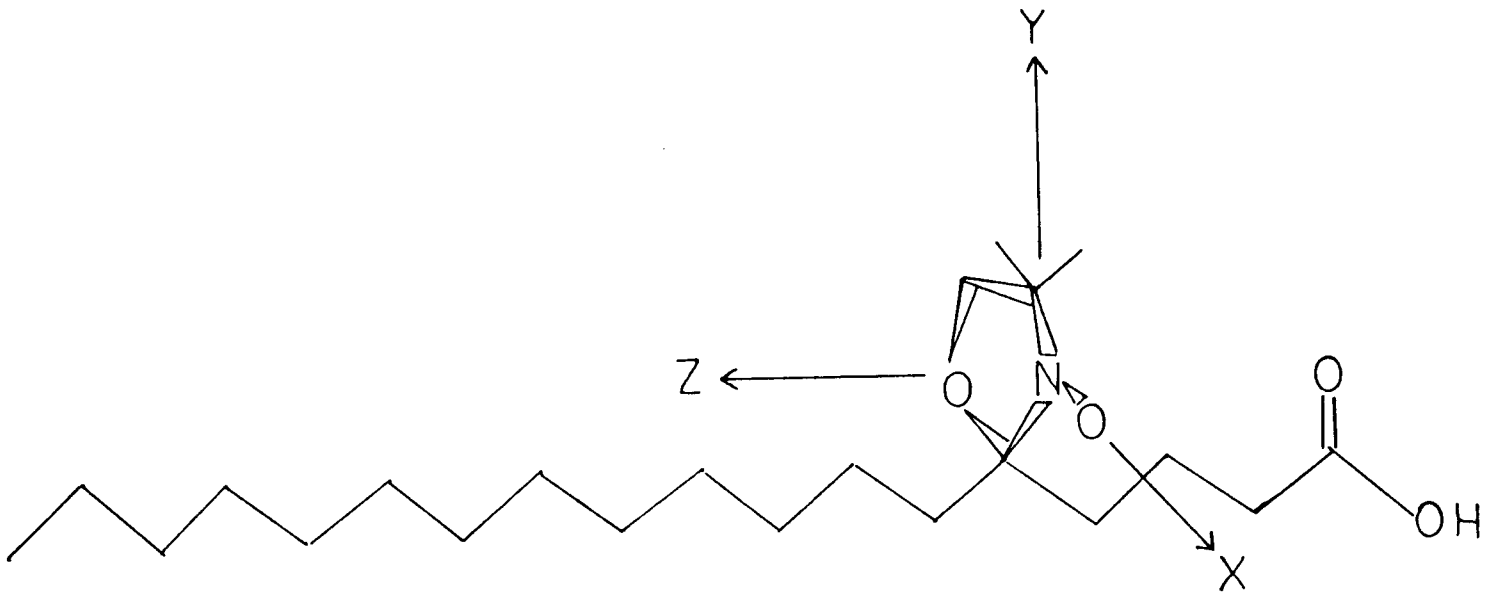

Figure 2.4 Structure of 5-doxyl stearic acid spin probe.

monitior the variation of $2T_{11}'$ (the separation between the outer extrema) which is linearly related to the order parameter [19].

$$2T_{11}' = 2a_o + (4S/3) \{ T_{zz} + (T_{xx} + T_{yy})/2 \} \qquad (2.10)$$

Where a_o is the isoptropic hyperfine coupling constant of the nitroxide free radical. From equation 2.12 when S decreases so does $2T_{11}'$. The interpretation of S and hence $2T_{11}'$ can be viewed as a measure of motional order. The change of $2T_{11}'$ with temperature can be evaluated as the variation of membrane fluidity with temperature.

Between the extremes of rapid motion and slow motion is the region of intermediate rates which is difficult to analyse. In this region none of the methods indicated above can be employed. In order to obtain useful information from this region of intermediate motion, spectral simulations are needed [19].

CHAPTER 3

EXPERIMENTAL

3.1 Preparation of 2,2,5,5-tetramethylpyrroline-1-oxyl-3-carboxylic Acid {V}.

The carboxylic acid spin label precursor {V} was prepared using the route illustrated below [26].

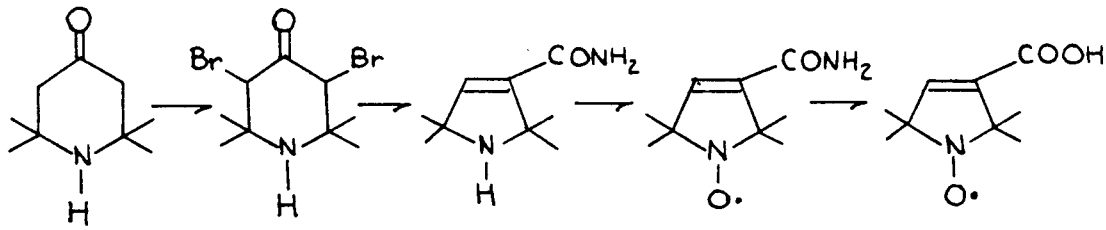

(I) (II) (III) (IV) (V)

The 2,2,6,6-tetramethyl-4-piperdone {I} was purchased from Aldrich and used without purification. The chemical modifications indicated above were carried out as follows:

Preparation of 3,5 dibromo-2,2,6,6-tetramethyl-4-piperidone hydrobromide {II}.

Compound {I} (4 g) was dissolved in glacial acetic acid (16 ml). Then with ice-water cooling and vigorous stirring, a solution of bromine (10 g) in glacial acetic acid (16 ml) was added. The reaction mixture was left to stand for a day. The

resultant precipitate was pressed out on a Buchner funnel, and washed successively with acetic acid, water and ether, and finally air-dried. The yield of crude {II} was 6.7 g (83%). This was used without additional purification.

Preparation of 2,2,5,5-tetramethylpyrroline-3-carboxyamide {III}.

With continous stirring, compound {II} (5 g) was added to a solution of 25% aqueous ammonia (50 ml), the resulting solution was subsequently saturated with KOH. The precipated crystals of {III} were collected and air dried. The yield of crude {III} was 2.2 g (82%). And on recrystallization from benzene gave a m.p. of 176-178°C (Lit. 178-179°C) was obtained.

Preparation of 3-carbamoyl-2,2,5,5-tetramethylpyrrolline-1-oxyl {IV}.

Compound {III} (2 g) was mixed with a solution of 30% hydrogen peroxide (5 ml), EDTA (0.11 g), and sodium tungstate (0.11 g) in distilled water (25 ml), and left in the dark at room temperature for 20 days. The resulting crystals was filtered and then air dried. The yield of crude free radical was 1.5 g (70%) [N.B. The yield of free radical is dependent on the freshness of the hydrogen peroxide]. Recrystallized from ethanol m.p. 197-200°C decomp. (Lit. 203-204°C decomp.).

Preparation of 2,2,5,5-tetramethylpyrroline-1-oxyl-3-carboxylic acid {V}.

The compound {IV} (1 g) was dissolved in a 10% sodium hydroxide solution (15 ml) and refluxed until the evolution of ammonia ceased. After cooling the solution, it was acidified with hydrochloric acid. The precipitate was filtered and dried. The yield of crude yellow crystalline acid-radical was 0.9 g (90 %). Recrystallized from benzene, the m.p. was 201-203°C (Lit. 210-211°C). A microanalysis (by Mr. P. Borda) of the compound {V} was done for carbon, hydrogen, and nitrogen content.

For $C_9H_{14}N_1O_3$:

Calculated	C: 58.68	H: 7.66	N: 7.60
Found	C: 58.26	H: 7.76	N: 7.54

3.2 Preparation of Spin Labelled Cardiolipin.

The spin labelled cardiolipin (SLCL) was prepared using the route illustrated below. For each SLCL preparation the compounds {VI} and {VII} were freshly prepared.

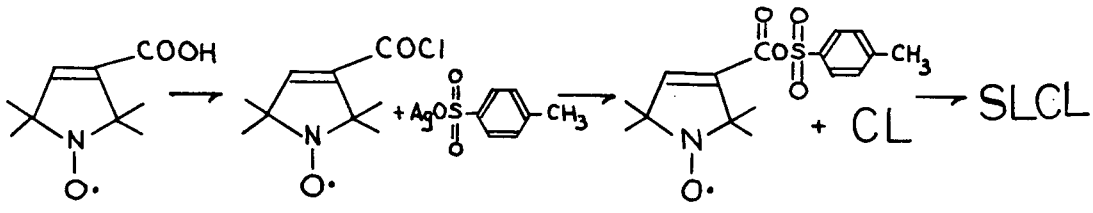

(V) (VI) (VII)

Preparation Of 2,2,5,5-tetramethylpyrroline-1-oxyl-3-carboxylchloride {VI} [26].

A suspension of compound {V} (0.5 g) in dry benzene (dried by refluxing over potassium and distilled) (6 ml) with freshly distilled dry pyridine (0.3 ml) cooled in a cold water bath was stirred under a nitrogen atmosphere. Then freshly distilled thionyl chloride (0.3 ml) in dry benzene (4 ml) was added dropwise to the resulting solution. The reaction mixture was stirred at room temperture for 1 hour. The salts which were formed were allowed to settle. The supernatant was decanted off into a sublimation chamber in a glove bag under nitrogen atmosphere. The solution was then evaporated to dryness under a stream of nitrogen gas. The residual crude acid chloride {VI} was then sublimed at 0.1 torr at 80°C to yield 0.4 g (73%) of dark-yellow crystals. The purity was confirmed by microanalysis (performed by Mr. P. Borda) of compound {VI}.

For $C_9H_{13}N_1O_2Cl$:

Calculated	C: 53.34	H: 6.46	N: 6.91
Found	C: 53.60	H: 6.74	N: 7.00

Preparation of (2,2,5,5-tetramethylpyrroline-1-oxyl-3-carboxyl)-p-toluenesulfonate {VII} [18].

In a glove bag under a nitrogen atmosphere, the sublimed acid chloride {VI} was washed into a dropping funnel with anhydrous dichloromethane (dried by refluxing with phosphorus pentoxide, followed by distillation). This was then added to a stirred suspension of silver tosylate in dry dichloromethane (1

ml) at 0°C under a nitrogen atmosphere. The mixture was stirred at 0°C for 30 minutes. The stirring was discontinued and the precipitate was allowed to settle. The anhydride in the supernatant was not isolated but used as it was.

Preparation of Spin Labelled Cardiolipin (SLCL) [18].

CL purchased from Sigma Chemical or Supelco Inc., was tested by TLC. Cardiolipin spotted on a silica gel-H TLC plate, developed in a solution of chloroform/methanol/water (65,25,4) showed a single spot [25]. The cardiolipin was therefore considered pure by this criteria.

To prepare the SLCL the cardiolipin was dried under a stream of nitrogen gas and was pumped on for 1 hour. The dried lipid film was disolved in dried dichloromethane. The chilled anhydride solution (about ten fold excess) was then added to the cardiolipin solution. The resulting reaction mixture was stirred under nitrogen and allowed to warm up to 25°C over a 2 hour period. The reaction mixture was then washed with water. The organic layer was withdrawn, dried and redissolved in chloroform.

The resulting mixture was divided and applied to two silica gel-H TLC plates. The plates were then chromatographed in a solution of ethylacetate/glacial acetic acid (96/4) [16]. The cardiolipin band Rf=0.05-0.10 was removed from the two plates, combined, and extracted with chloroform/methanol (1/2). The SLCL solution was dried and redissolved in chloroform. A 20 micro-litre sample was degassed and an ESR spectrum was recorded to determine the ratio of the height of the high field line to the

height of the central field line. This ratio is indicative of the motion of the spin probe when it is attached to the cardiolipin. After the initial ESR test, the crude SLCL solution was subjected to TLC again. The TLC step was repeated until the ESR line ratio was constant. The yield of SLCL was about 5% as indicated by integration of ESR spectra.

3.3 Determination of Spin Hamiltonian Parameters of {V} and Control Experiments.

The spin Hamiltonian parameters (T and g) of the spin label {VI} in 30% glycerol and D_2O were determined in a low temperature study. In addition ESR spectra of the spin probe were recorded in the presence of buffered solution containing Na^+, Ca^{2+}, cardiolipin in the lamellar phase and cardiolipin in the hexagonal phase at room temperature for control purposes. In addition ESR spectra were recorded of the spin probe in chloroform and chloroform with cardiolipin.

3.4 Sample Preparation.

In both 5-doxyl-stearic acid spin probe and spin labelled cardiolipin experiments the ratio of spin labelled molecule to cardiolipin was adjusted to 1:100. In the case of the stearic acid probe experiments, this was done by adding the correct volume of a stock solution ($5X10^{-3}M$) of spin probe. For the spin labelled cardiolipin experiment this was done by integrating the centre field line and comparing it to standards and then diluting with cardiolipin to the desired concentration.

Following this the solvent was removed using a gentle stream of nitrogen gas, the resulting film was pumped on for 1 hour at 0.1 torr to remove all traces of solvent.

Preparation of Lamellar Phase.

The dried lipid (see above) was then dispersed in 50-100 micro-litre of buffer(100mM EDTA, 100mM NaCl, 110mM tris-HCl pH 7.3). The lamellar phase was formed by vortexing until the lipid was dispersed. The addition of EDTA to the buffer is to prevent the formation of the hexagonal phase or any other phase induced by divalent cations that may be present in the cardiolipin as an impurity. The volume of buffer used consequently, depended on the variable divalent ion content of the commercially bought lipid [11].

Preparation of Hexagonal Phase.

The cardiolipin, together with the spin probe (100:1) was first dispersed as the lamellar phase. Subsequently the hexagonal phase was produced, by adding buffered Ca^{2+} solution (100mM $CaCl_2$, 50mM tris-HCl pH 7.3) until a one to one mole ratio of Ca^{2+} to cardiolipin was achieved.

Titration of Lamellar Phase with Ca^{2+} buffer to yield Hexagonal Phase.

These experiments were carried out with the stearic acid probe. The sample was first dispersed into the lamellar phase. Then incremental amounts (10-20 %) of Ca^{2+} buffer (100mM $CaCl_2$,

50mM tris-HCl) were added. The sample was vortexed for 20 minutes to yield an uniform mixture. Then ESR spectra of the sample were recorded as a function of temperature from 20-50°C at 3-5°C intervals. The above procedure was repeated until a one to one mole ratio of Ca^{2+}/cardiolipin was reached.

Spin Probe studies of cardiolipin in the presence of excess Ca^{2+}.

Two approaches were used to study the effect of excess Ca^{2+} on the hexagonal phase. In one, the buffered Ca^{2+} solution concentration was kept constant and the cardiolipin concentration was varied. In the other set of experiments the situation was reversed, the cardiolipin concentration was kept constant and the Ca^{2+} concentration was varied.

A cardiolipin sample (5 mg) was first dispersed to the lamellar phase and then precepitated by addition of equal mole % of Ca^{2+} [0.1M] as in preparation of hexagonal phase (cardiolipin concentration [0.1M]). ESR spectra were then recorded as a function of temperature for the sample and for subsequent samples. After the ESR study the sample was diluted in 5 times the initial volume of buffered Ca^{2+} solution to give a mole ratio of 1 to 5 cardiolipin/Ca^{2+} (cardiolipin [0.02M]). Then the sample was again diluted, to 15 times the initial volume to give a ratio of 1 to 15 cardiolipin/Ca^{2+} (cardiolipin [6.7mM]).

In the second set of experiments the cardiolipin concentration was kept constant [6.7mM] by having cardiolipin (5 mg) dispersed in buffer (0.5 ml) of different Ca^{2+} concentrations. The concentration of Ca^{2+} used were 0.1M, 0.5M,

1.0M, 2.5M, and 5.0M with cardiolipin to Ca^{2+} ration of 1 to 15, 75, 150, 375, and 750 respectively.

3.5 Manipulation of samples.

ESR samples of the lamellar phases and non-precipitated material were taken up in one to three 20 micro-litre disposable pipets. For the hexagonal phases and precipitated samples a 100 micro-litre pipet was used. To load the micro pipets the sample was taken up by suction and the other end of the pipet was thermally sealed. The sample, after cooling the tube, was then centrifuged down to the sealed end.

3.6 The Recording of ESR spectra.

All ESR spectra were recorded on an ESR spectrometer which consisted of: a Varian 12" magnet with a Mk II field-dial control, an Hewlett-Packard klystron power supply and sweep unit, a home-built AFC and 100 kHz modulation unit and an Ithaco 391A phase-lock amplifier. The microwave bridge was a reflective homodyne type using a TE 102 cavity, three port circulator, Schottky detector diode and a microwave bucking arm. The cavity was fitted with a dewar system and the temperature controlled to ±0.1°C using a Varian temperature control unit. The temperature was measured by means of a copper-constantan thermocouple inserted into the cavity. The magnetic field was calibrated with a home-built proton magnetometer. The spectra, along with calibration data, were recorded using a Hewlett-Packard X-Y recorder.

CHAPTER 4

RESULTS

4.1 Spin probe studies of cardiolipin in the Lamellar Phase.

The spin probe 5-doxyl-stearic acid was incorporated into the lamellar phase of cardiolipin as described in Chapter 3. ESR spectra were recorded over the temperature range 5-50°C at 3-5°C intervals. The ESR spectra of 5-doxyl-stearic acid in the lamellar phase of cardiolipin at various temperature is illustrated in figure 4.1. Spectra obtained were the slow motion type which could be analysed in terms of the order parameter S or the apparant hyperfine coupling T_{11}'. The temperature dependence of T_{11}' is shown in figure 4.2. The temperature profile shows a discontinuity at 37°C which can be attributed to the thermotropic phase transition of the disodium cardiolipin [28]. Results obtained from this study are in agreement with the results obtained by Hegner et al.

4.2 Spin probe studies of cardiolipin in Hexagonal Phase.

ESR spectra were recorded for 5-doxyl-stearic acid incorporated in the cardiolipin hexagonal phase over the temperature range 3-55°C at 3-5°C intervals. Figure 4.3 shows spectra of the spin probe in the Ca^{2+} complexed cardiolipin precipitates at various temperatures. These spectra show an increase in the amount of hyperfine splitting T_{11}' which signifies a decrease in the motional freedom of the probe. The T_{11}' were

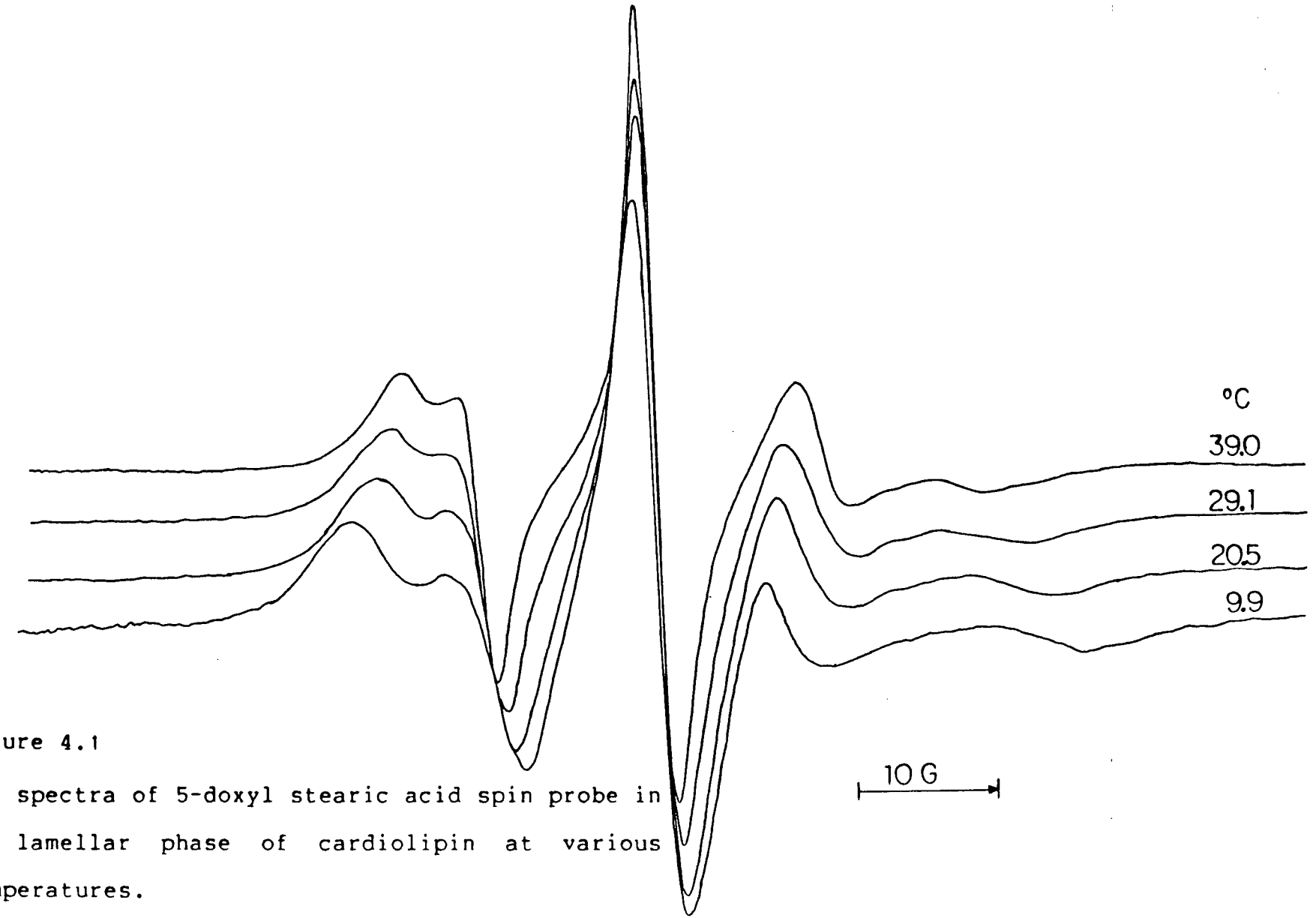

Figure 4.1

ESR spectra of 5-doxyl stearic acid spin probe in the lamellar phase of cardiolipin at various temperatures.

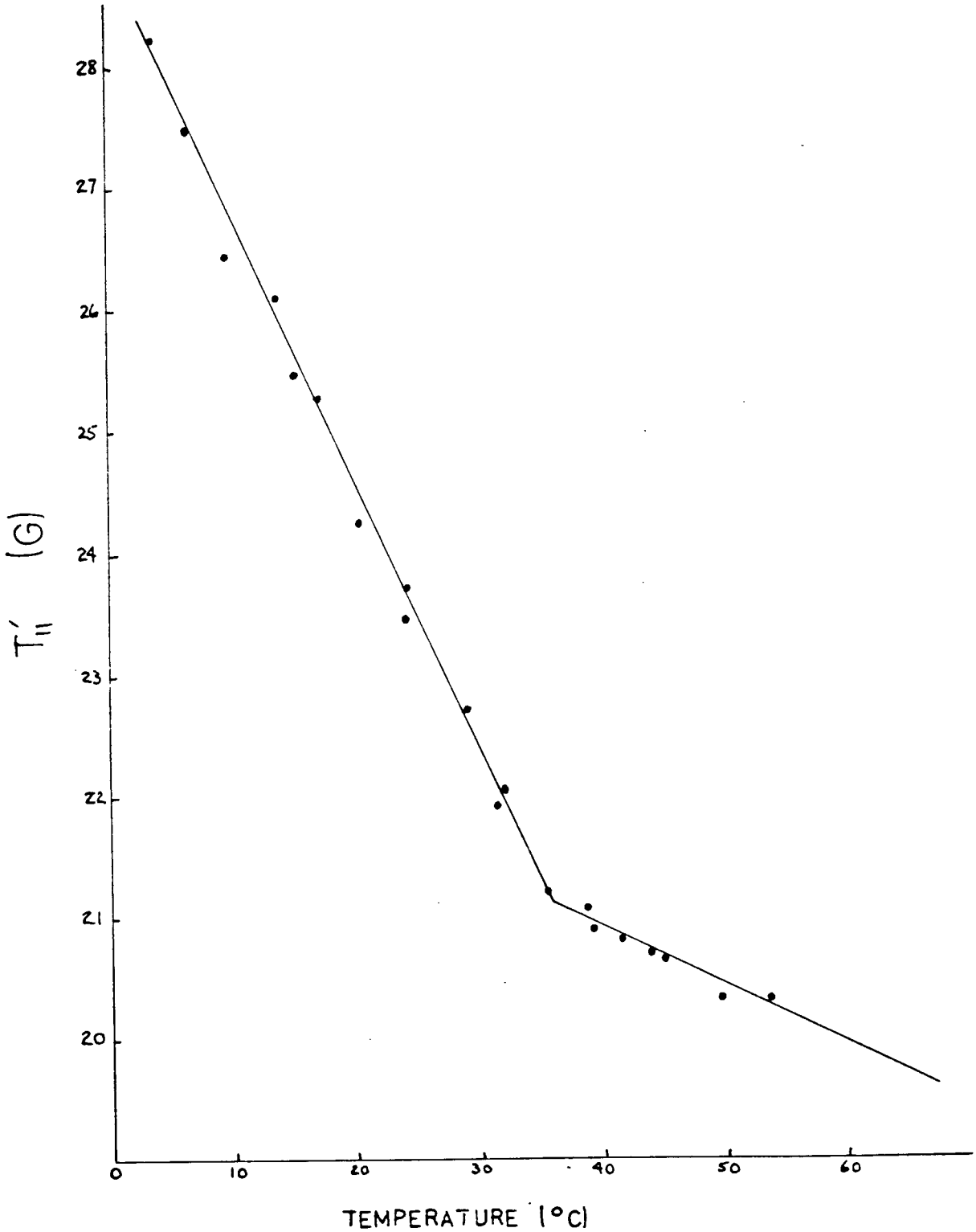

Figure 4.2 Temperature dependence of T'_{11} of 5-doxyl stearic acid spin probe in the cardiolipin lamellar phase.

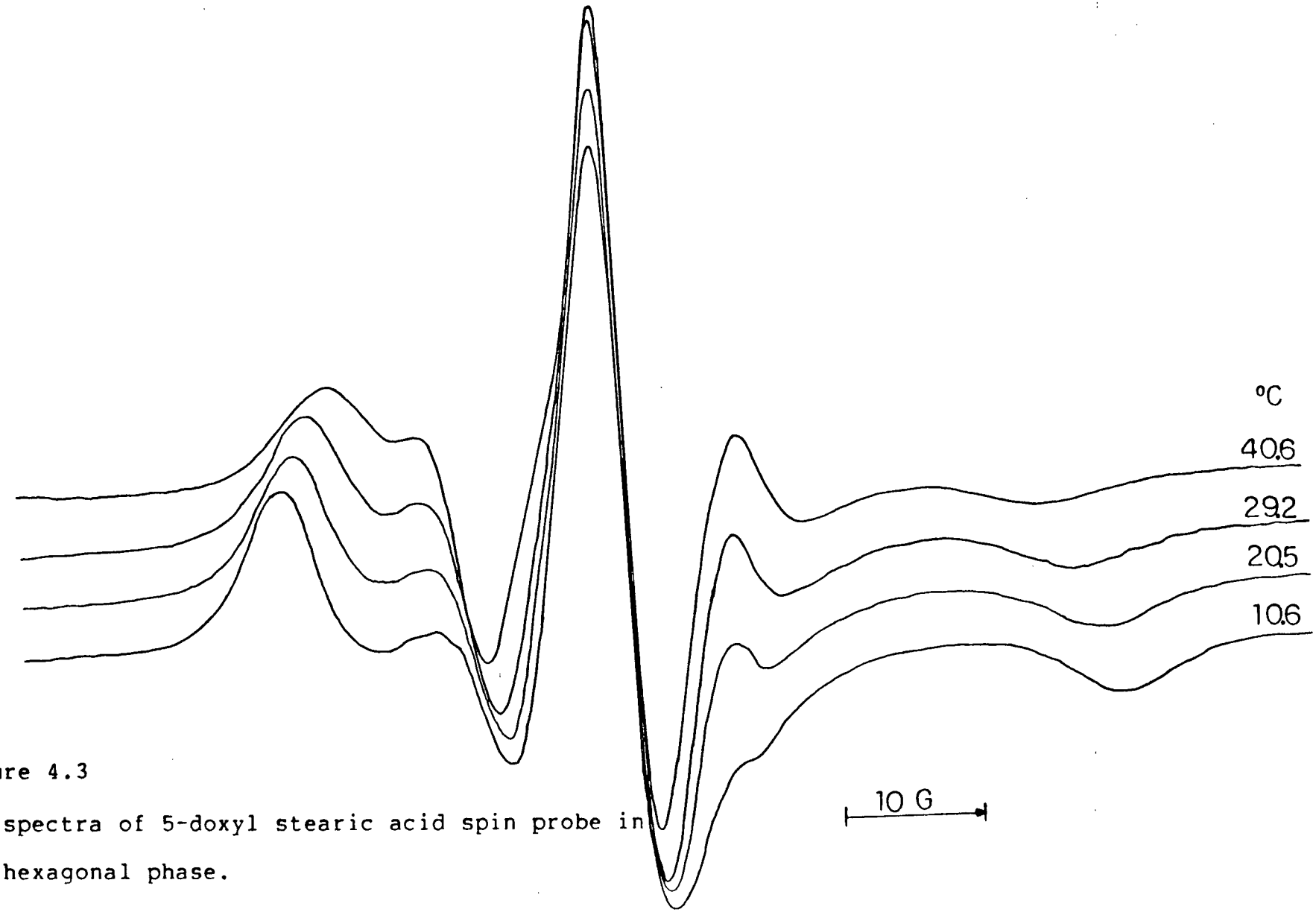

Figure 4.3

ESR spectra of 5-doxyl stearic acid spin probe in the hexagonal phase.

measured and are plotted against temperature in figure 4.4. No discontinuity was observed, which was expected since the thermotropic phase transition of the calcium cardiolipin is 90°C [28]. On the same plot is the temperature profile of the spin probe in the lamellar phase of cardiolipin to illustrate the difference between the lamellar and hexagonal phase as monitored by the spin probe. This result is again in agreement with Hegner et al [14].

4.3 Spin Probe Studies of Mixed phases.

To further study the lamellar to hexagonal phase transition, a titration experiment was performed. In these experiments the lamellar dispersions were titrated with buffered Ca^{2+} solution until one to one Ca^{2+} to cardiolipin mole ratio or 50 mole % of Ca^{2+} was added. ESR spectra at various temperatures were recorded for each step of the Ca^{2+} titration experiment to yield the hexagonal phase from the lamellar phase. A temperature profile was obtained for the spin probe in the cardiolipin environment with 9, 17, 29, 38, 41, 47 and 50 mole % of buffered Ca^{2+} solution.

The spectra of the spin probe in the lamellar phase in the presence of 17 mole % of Ca^{2+} at different temperatures are illustrated in figure 4.5. These spectra show the T'_{11} obtained was larger than those for the lamellar phase in the absence of Ca^{2+} indicating a more ordered environment. The same results were obtained by dispersing commercial cardiolipin in buffered Na^{+} solution containing no EDTA to chelate any Ca^{2+} present. This indicates the small amount of Ca^{2+} or divalent impurity

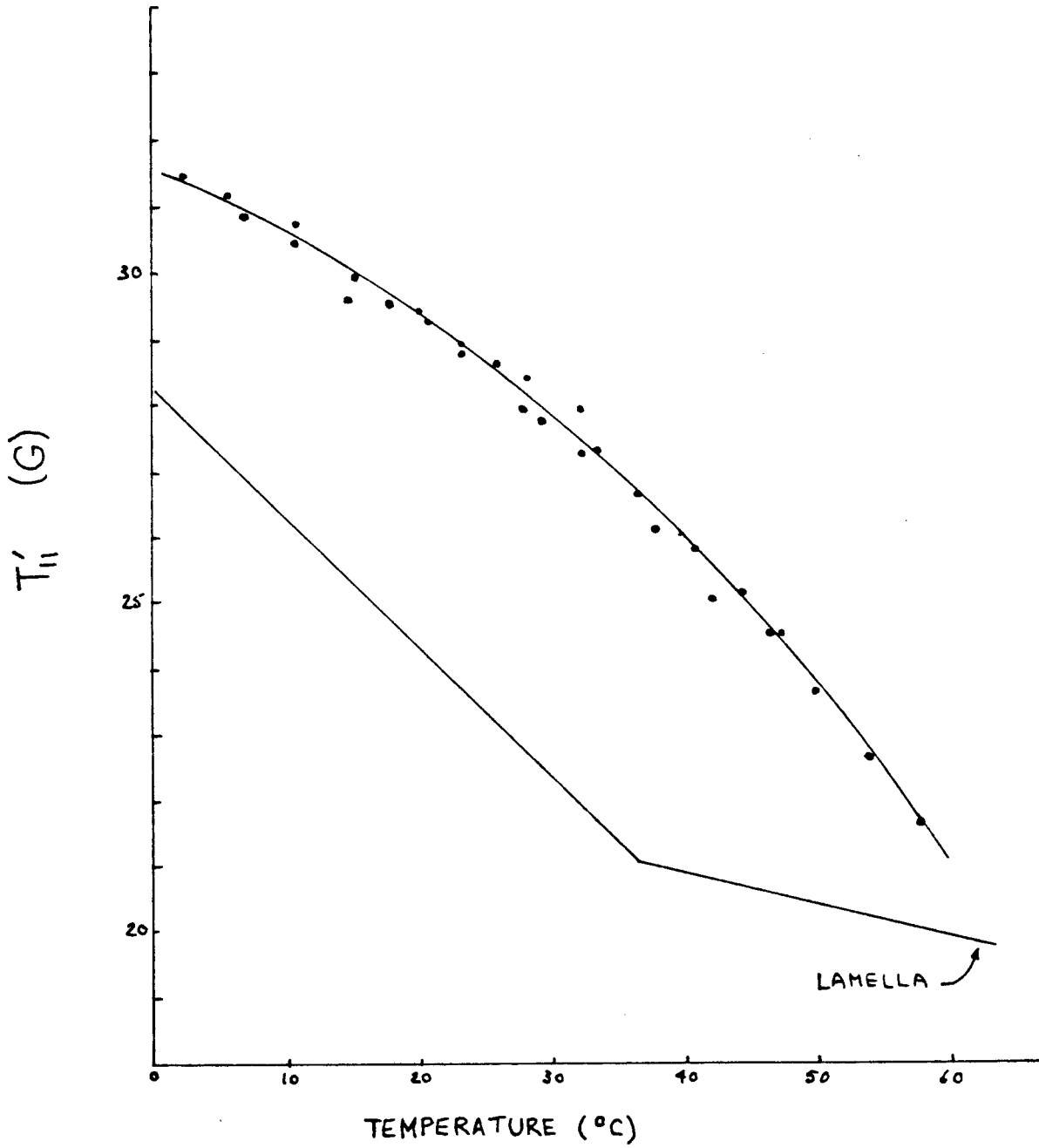

Figure 4.4 Temperature dependence of T'_{11} of 5-doxyl stearic acid spin probe in the cardiolipin hexagonal phase.

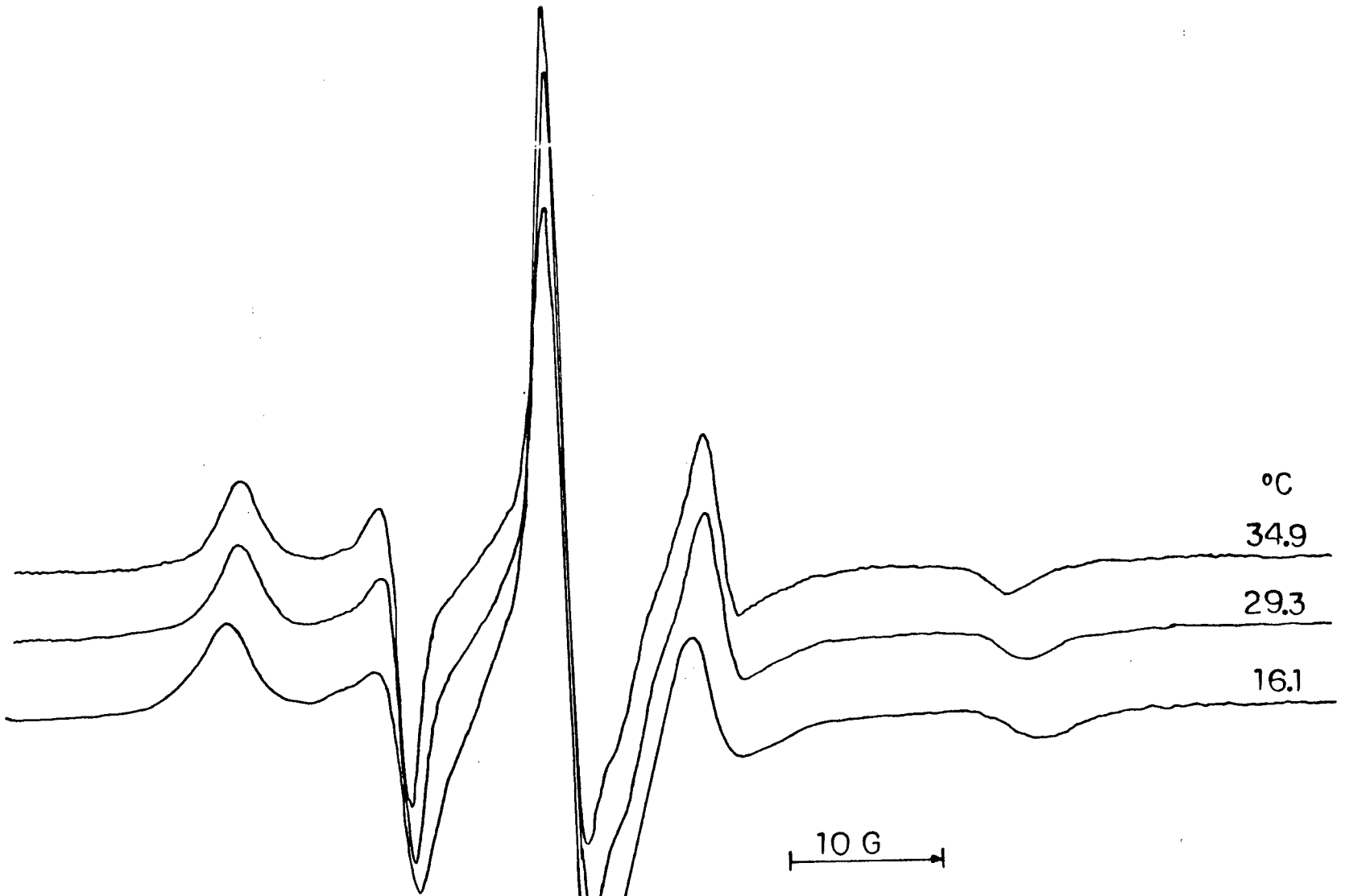

Figure 4.5 ESR spectra of 5-doxyl stearic acid spin probe in the 'ordered lamellar phase'.

present in the commercially bought cardiolipin [11] is enough to order the lamellar phase. The T_{II}' was measured and plotted against temperature in figure 4.6 for the different mole % of Ca^{2+} added. The results of the lamellar and hexgonal phases are outlined to show the difference between the three sets of experiments. No precipitation was evident until about 38 mole % of Ca^{2+} were added to the sample. Between 9-29 mole % of Ca^{2+} added the hyperfine splitting at high temperature approaches those of the hexagonal phase and exceed them above 50°C. This observation will be discussed later.

The titration experiment results also showed that between the Ca^{2+} concentration of 9 and 38 mole % we can resolve two overlapped spectra above 40°C. A resolved spectrum is illustrated in figure 4.7. The T_{II}' of the resolved spectrum corresponds to the T_{II}' of the 5-doxyl-stearic acid probe in the lamellar phase at the same temperature. This shows that the spin probe is monitoring two different environments.

4.4 ESR Spin Probe Studies of the Hexagonal Phase in the Presence of Excess Ca^{2+}.

In a further set of experiments the hexagonal phase of cardiolipin is subjected to an excess amount of Ca^{2+}. Two routes were used for this as indicated in section 3. No noticable difference was observed in the T_{II}' measurement when the Ca^{2+} concentration was kept constant at 0.1M with the cardiolipin concentration varied from 0.1M to 6.7mM.

Alternatively when the concentration of cardiolipin was kept constant at 6.7mM and the concentration of Ca^{2+} varied from

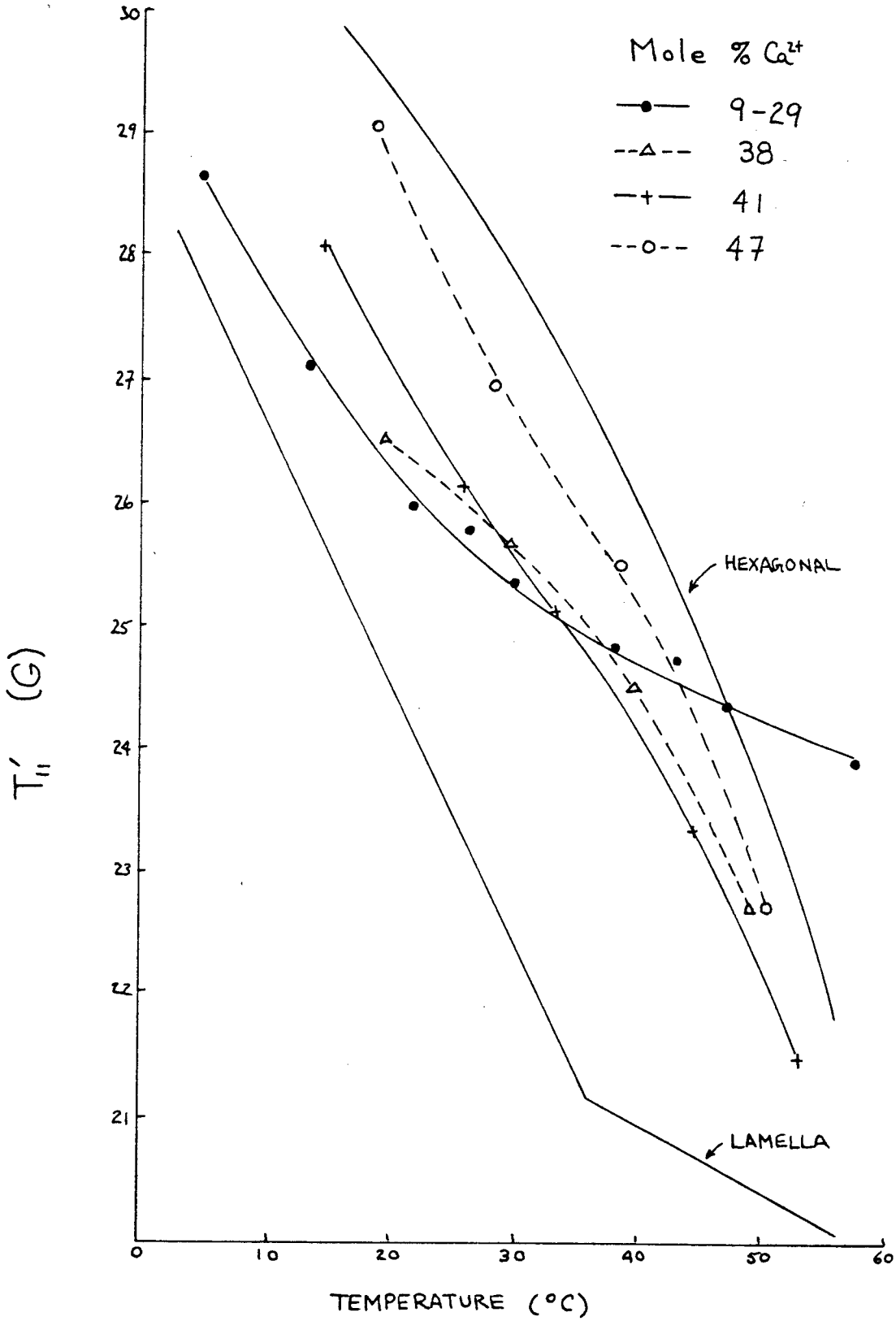

Figure 4.6 T'_{11} vs temperature for 5-doxyl stearic acid spin probe in the lamellar phase with various mole % of Ca^{2+}.

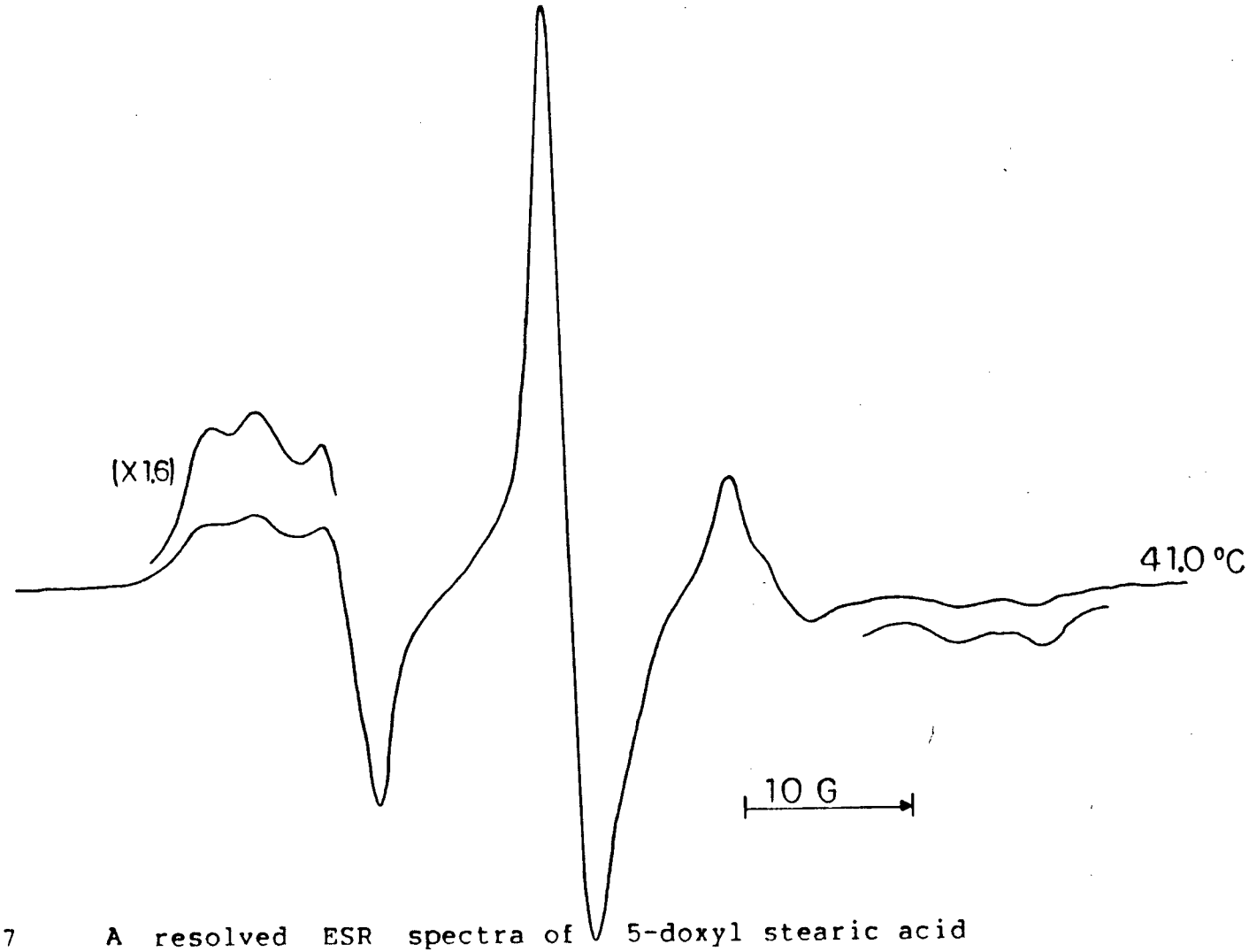

Figure 4.7 A resolved ESR spectra of 5-doxyl stearic acid spin probe in the mixed phase.

0.1M to 5.0M, a large change was observed in the value of T'_{11}. ESR spectra recorded at about 20°C for each of the five concentrations of Ca^{2+} are illustrated in figure 4.8. ESR spectra were recorded as a function of temperature at each Ca^{2+} concentration. The vaules of T'_{11} were obtained and plotted as a function of temperature in figure 4.9. The results show when Ca^{2+} concentration was increased the T'_{11} also increased indicating an increase in order.

4.5 The Determination of Spin Hamiltonian Parameters.

The spin Hamiltonian parameters of {V} were determined in a low temperature study. These parameters are needed for the calculation of correlation times and for determining the rigid limit of the spin label. The temperature which gave the most well resolved spectrum of spin probe {V} in 30% glycerol and D_2O was -57.5°C. From the spectrum the apparent T and g values were measured. These values were used as the starting point for simulating the spectrum to find more accurate T and g values for spin probe {V}. The experimental and the simulated spectra are shown in figure 4.10, and 4.11 respectively. The spin Hamiltonian parameters used in the simulation shown in figure 4.11 are listed below:

T_{11} = 36.8 G $\qquad$ g_{11} =2.0017

$T_{\perp}$ = 5.8 G $\qquad$ $g_{\perp}$ =2.0069

The spectral simulations were performed using computer programmes written by J. C. Tait [36].

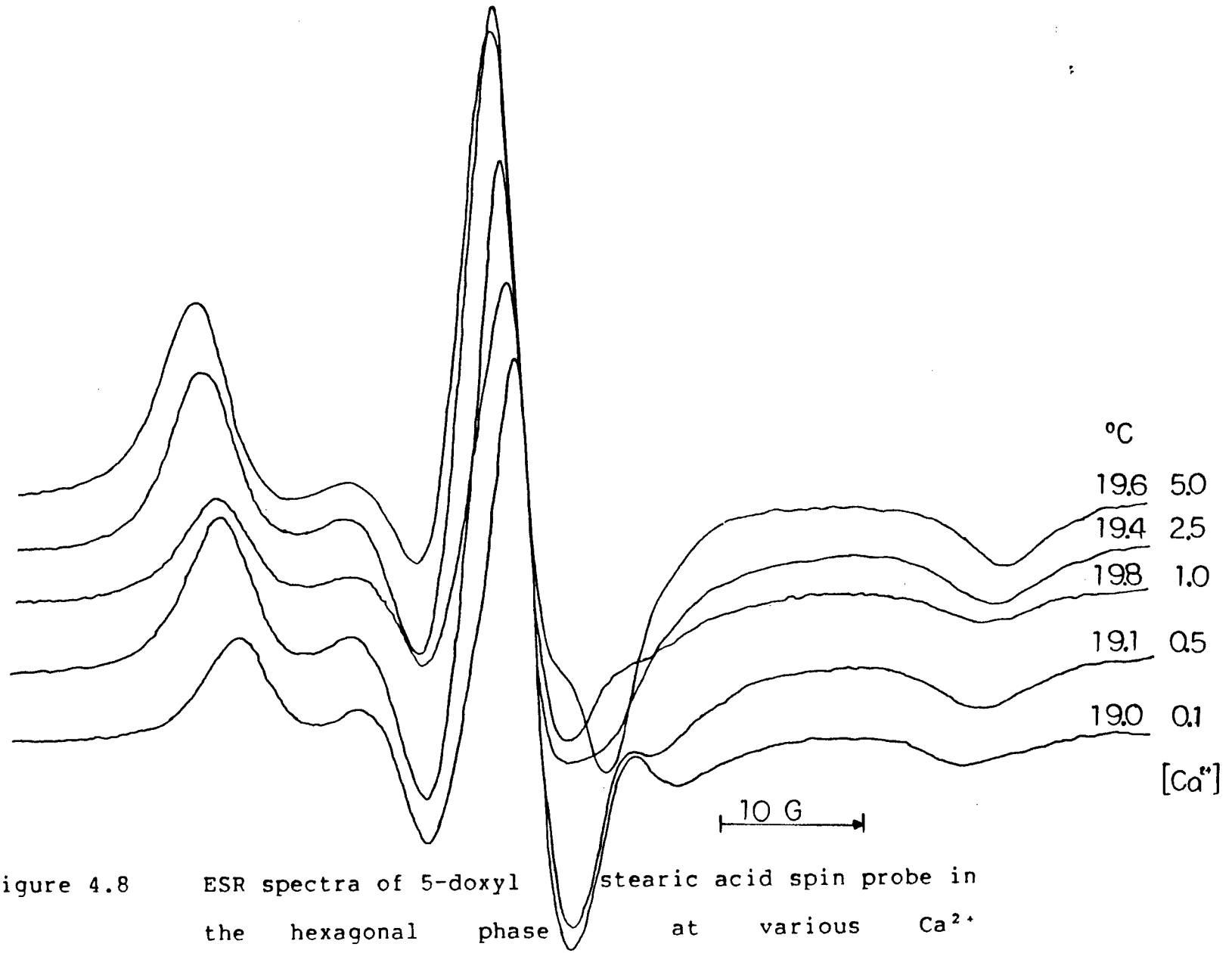

Figure 4.8 ESR spectra of 5-doxyl stearic acid spin probe in the hexagonal phase at various Ca^{2+} concentrations.

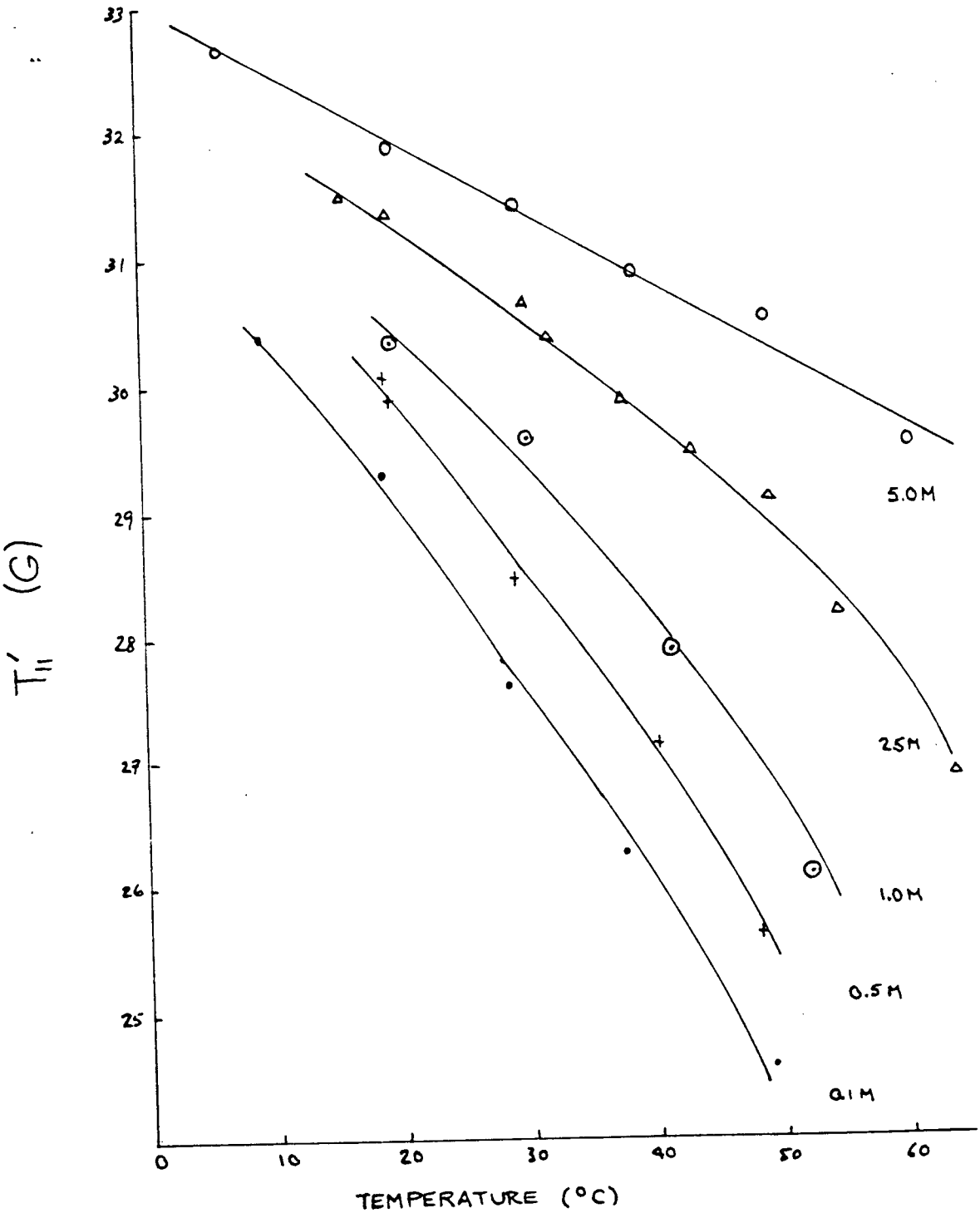

Figure 4.9 T'_{II} vs temperature of 5-doxyl stearic acid spin probe in the hexagonal phase at various Ca^{2+} concentrations.

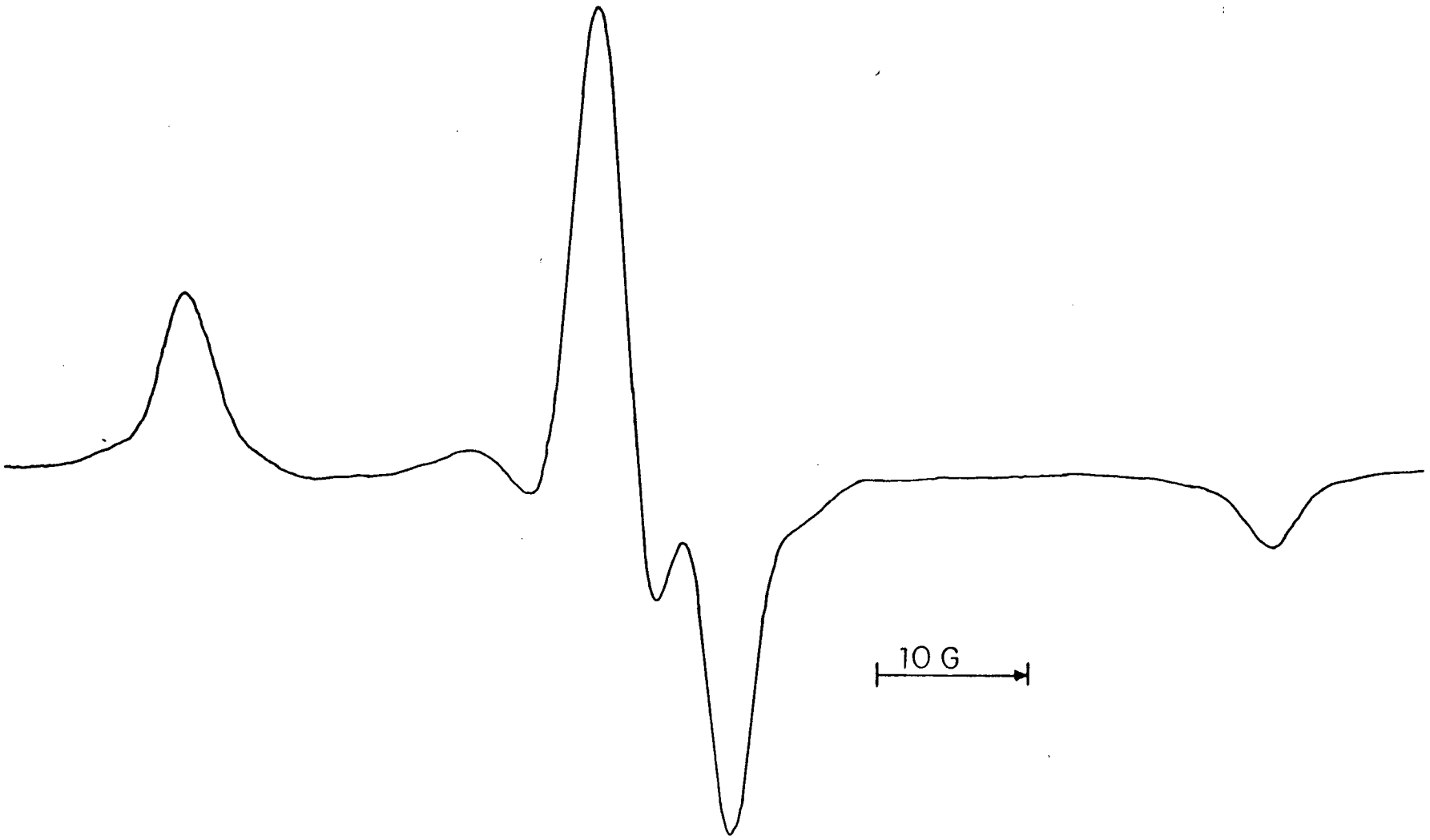

Figure 4.10 ESR spectrum of spin probe {V} in 30% glycerol and D_2O.

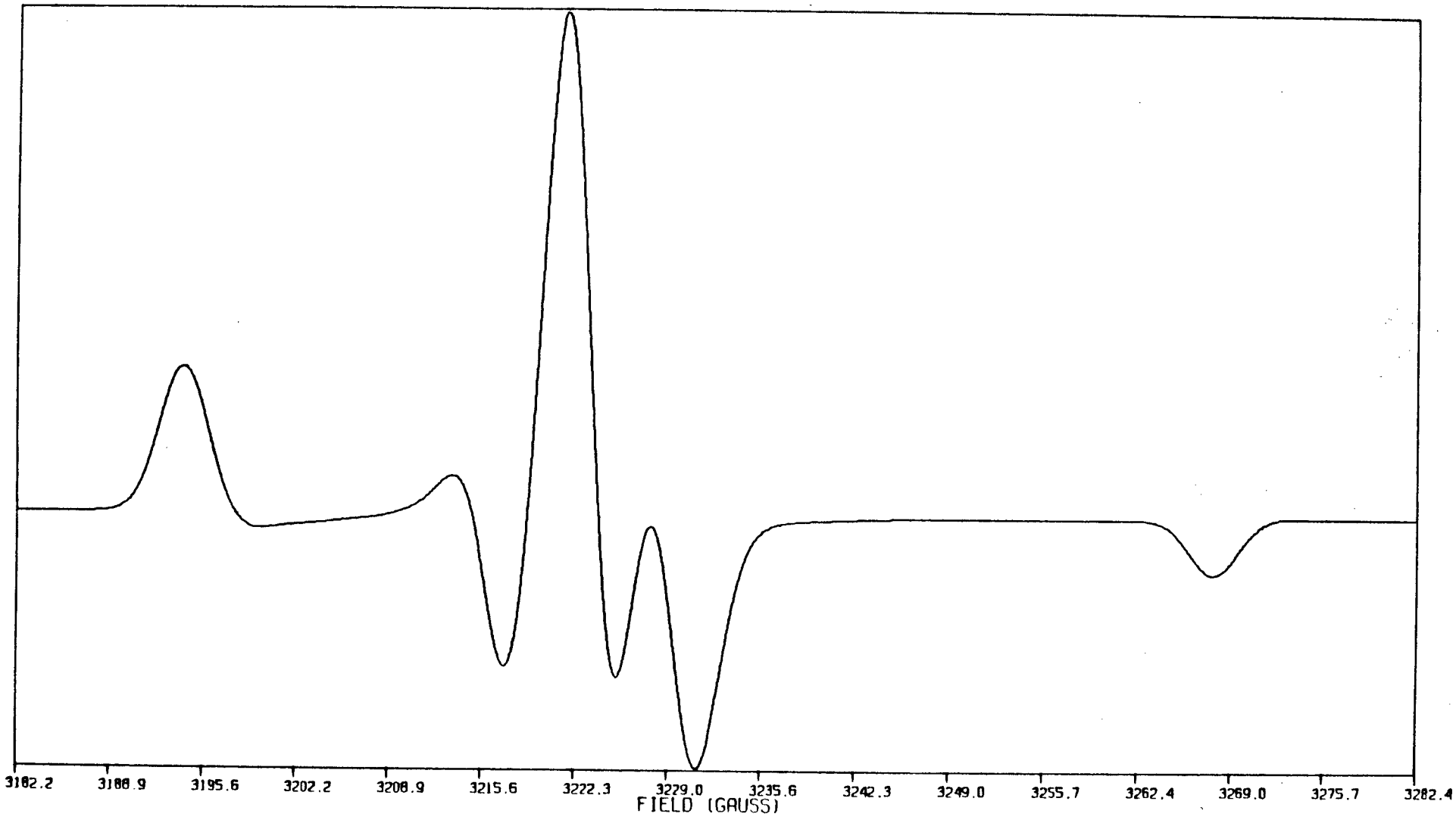

Figure 4.11 Simulated spectrum of spin probe {V} in 30% glycerol and D_2O.

4.6 Control studies of spin probe {V}.

The ESR spectra of spin probe {V} in control studies were recorded at room temperature. The control studies for spin probe {V} are as follow: in chloroform, chloroform containing cardiolipin, a buffered solution containing Na^+ (0.1M pH 7.2), a buffered solution containing Ca^{2+} (0.1M pH 7.3), cardiolipin lamellar phase, and cardiolipin hexagonal phase. The six spectra were simliar and consisted of three narrow lines of almost equal intensity. A typical spectrum is shown in figure 4.12. The three line heights and the linewidth of the mid field line were measured and their τ_B and τ_C calculated using the equation (2.6, 2.7) in Chapter 2. The τ_B and τ_C calculated for the six control studies for the spin probe {V} are in table 4.1.

4.7 SLCL in Chloroform.

ESR spectra of SLCL in chloroform were recorded to test the purity of the SLCL for contamination from unreacted spin label before use in ESR studies. A spectrum of SLCL in chloroform is shown in figure 4.13. In the preparation of the SLCL the TLC of the crude SLCL was repeated until the ratio (R) of the high field line to the mid field line was constant. The ratio obtained for purified SLCL was R=0.65 as compared to R of almost equal to one for the spin probe {V} in solution. The smaller the ratio (R) of high field line to central line the less unreacted spin label is present. During the tests to determine the purity of the SLCL, the ratio R increase with the exposure to high temperatures and length of time after TLC. This indicates the

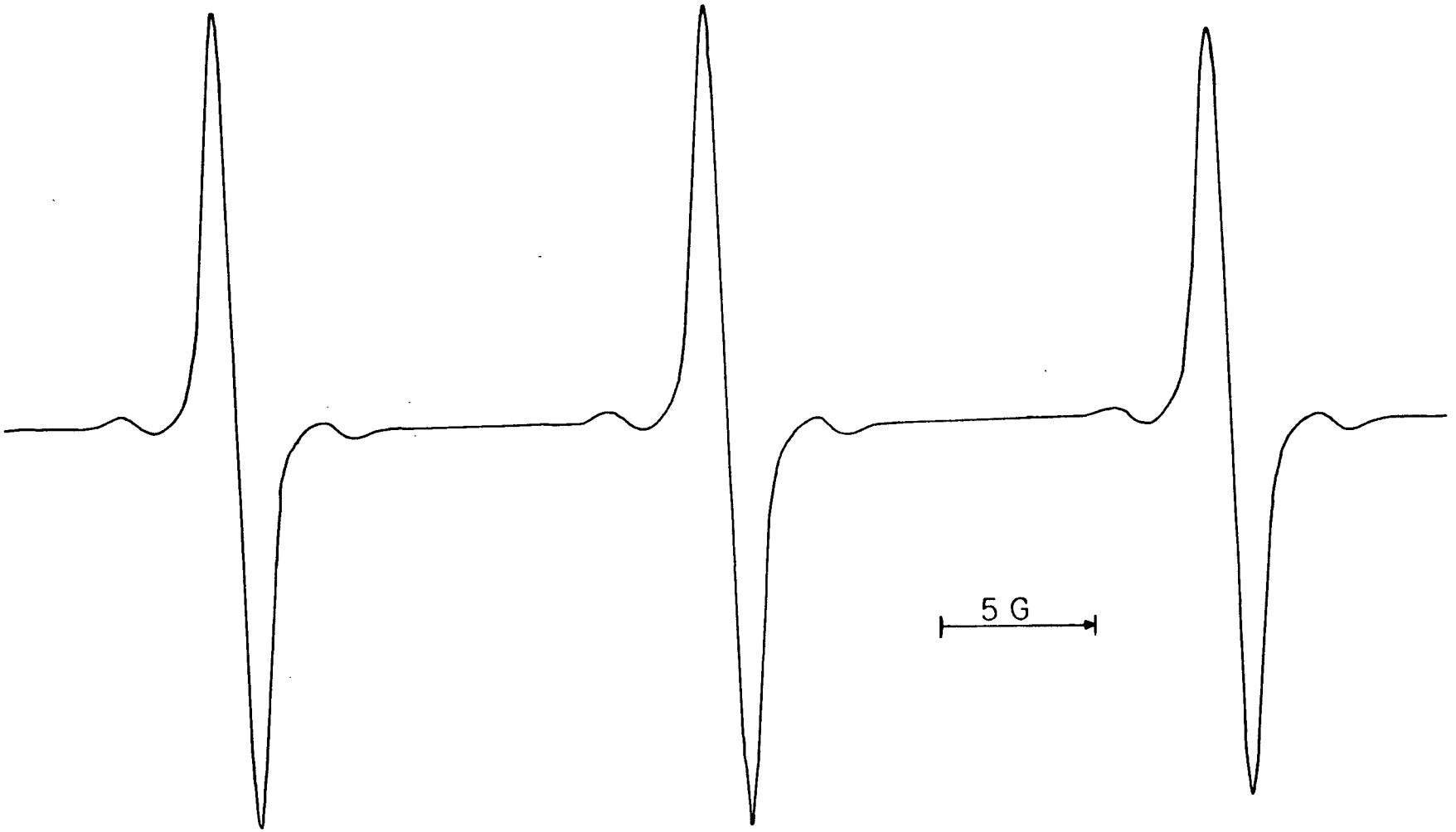

Figure 4.12 ESR spectrum of spin probe {V} in chloroform solution.

Table 4.1

Medium	(s)	(s)
Chloroform Solution	$2.40X10^{-11}$	$2.79X10^{-11}$
Chloroform Solution with Cardiolipin	$4.02X10^{-11}$	$4.04X10^{-11}$
Buffered Aqueous Na^{+} Solution	$1.52X10^{-11}$	$2.19X10^{-11}$
Buffered Aqueous Ca^{2+} Solution	$1.93X10^{-11}$	$3.50X10^{-11}$
Lamellar Phase of Cardiolipin in Buffered Aqueous Na^{+} Solution	$1.40X10^{-11}$	$2.08X10^{-11}$
Hexagonal Phase of Cardiolipin in Buffered Aqueous Ca^{2+} Solution	$1.59X10^{-11}$	$2.91X10^{-11}$

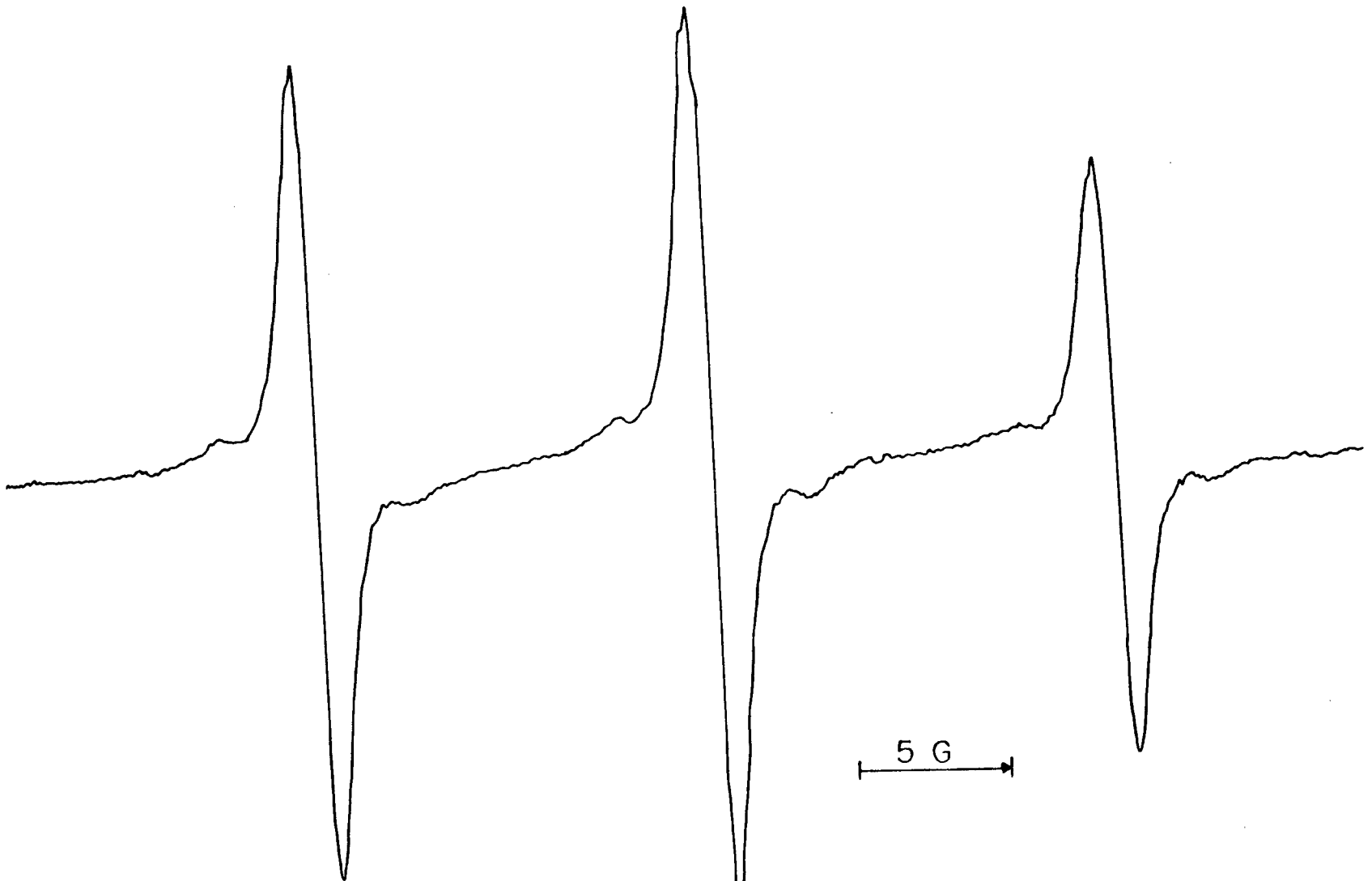

Figure 4.13 ESR spectrum of spin labelled cardiolipin in chloroform solution.

SLCL is not a very stable molecule. The spin moiety tends to fall off the cardiolipin moleccule with exposure to high temperature and extended length of time after it had been TLC.

4.8 SLCL in Lamellar Phase.

ESR spectra of the spin labelled cardiolipin in the lamellar structure (100:1 unlabelled to labelled) were recorded for the temperature range 3-35°C at 3-5°C intervals. The spectra obtained as shown in figure 4.14 consist of three narrow lines indicating the spin label to be in rapid motion. The three line heights and the linewidth of the mid field line were measured for each spectrum at each temperature and the correlation times calculated as described in Chapter 2. The correlation times (τ_B and τ_C) were plotted against temperature (Figure 4.15) which showed a smooth decrease of correlation time with temperature. This result was expected since the SLCL nitroxide moiety is at the head group and is monitoring the aqueous environment above the bilayer.

4.9 SLCL in Hexagonal Phase.

The ESR spectra of SLCL in the hexagonal phase is drastically changed from the ESR lineshape observed of SLCL in the lamellar phase reflecting much less mobility of the probe. ESR spectra were recorded for the temperature range 5-50°C in 3-5°C interval. ESR spectra of SLCL in hexagonal phase of cardiolipin at several temperatures are illustrated in figure 4.16. The lineshape is no longer the three narrow lines as

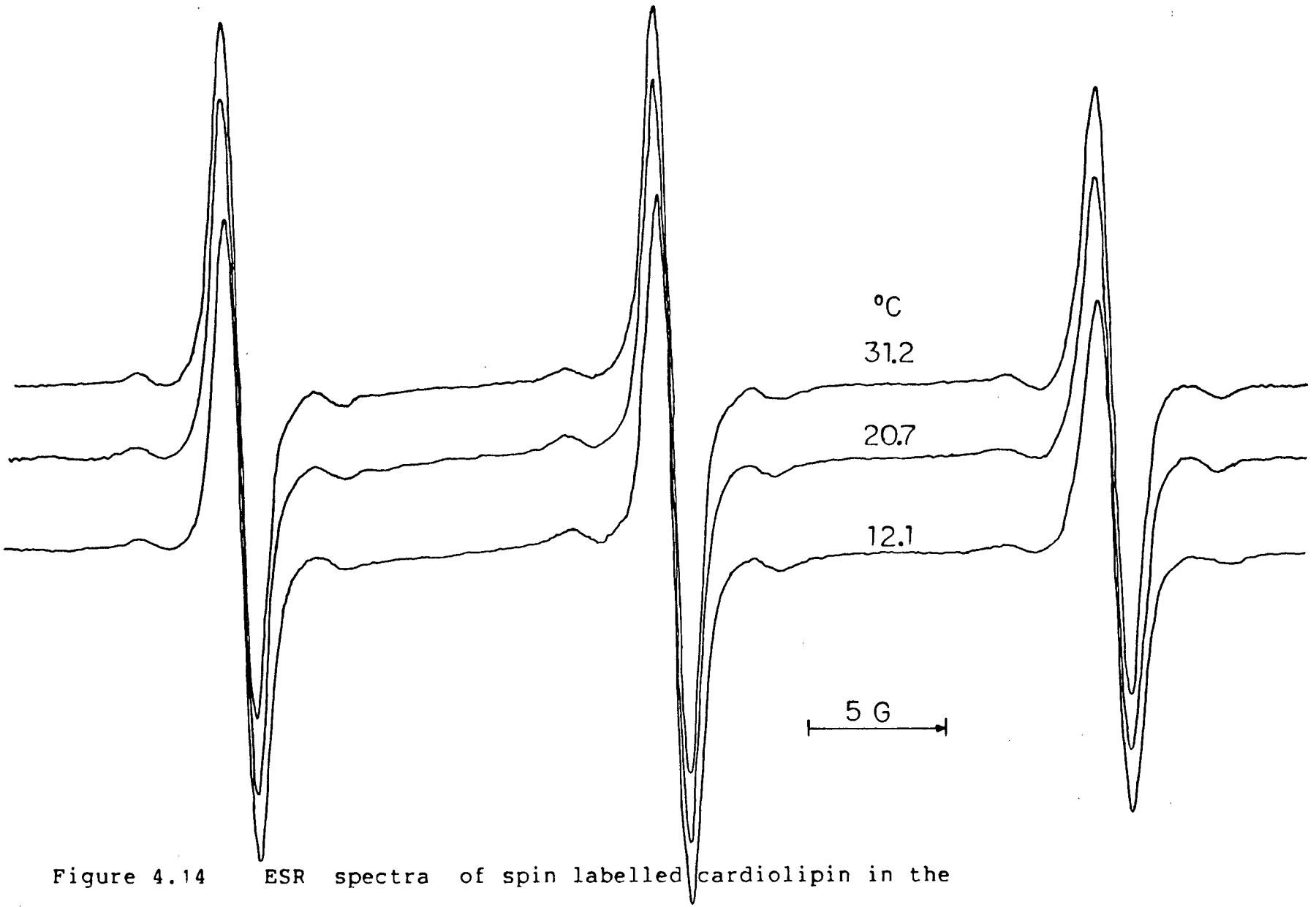

Figure 4.14 ESR spectra of spin labelled cardiolipin in the lamellar phase.

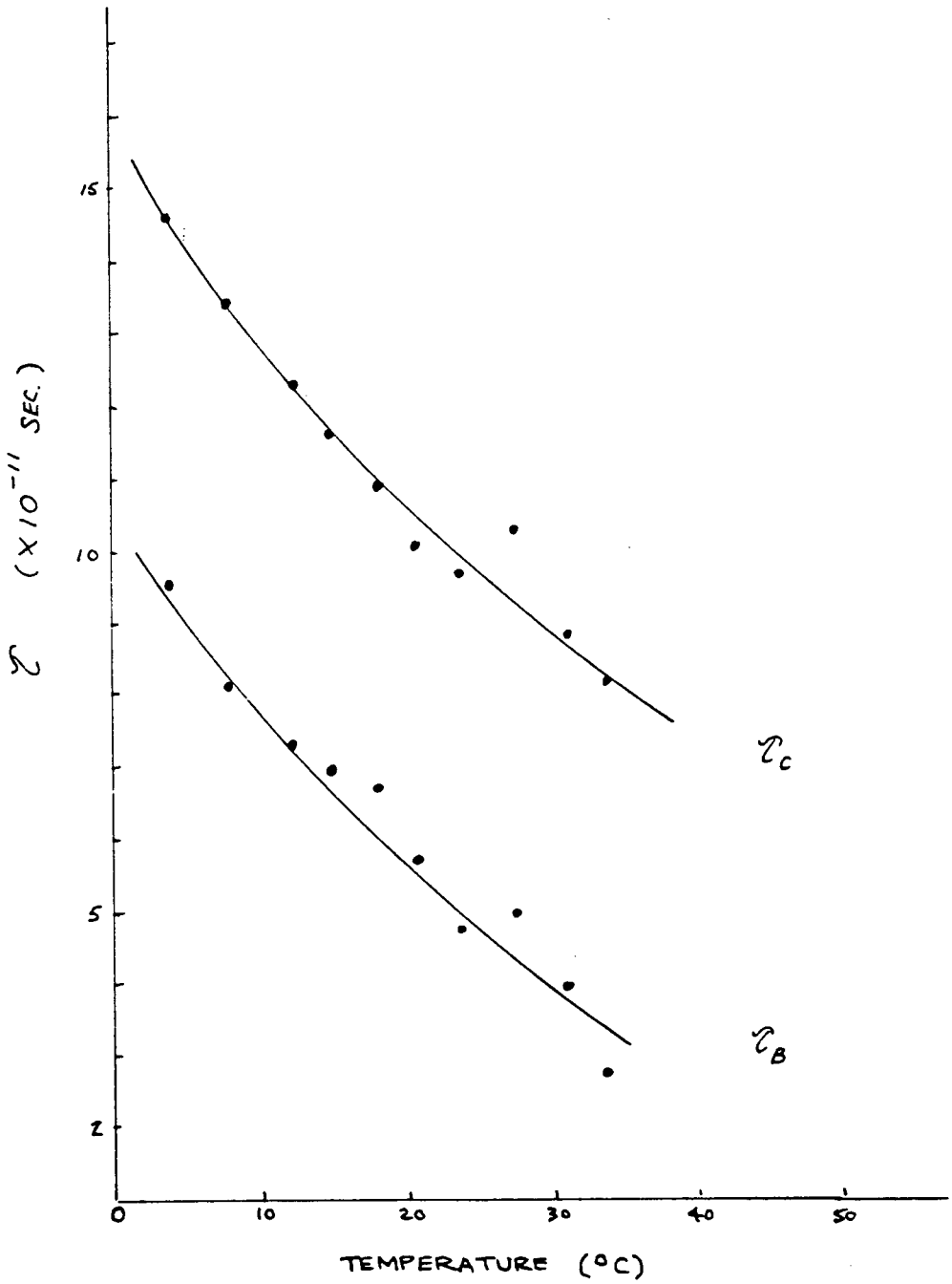

Figure 4.15 τ_B and τ_C vs temperature for SLCL in the lamellar phase.

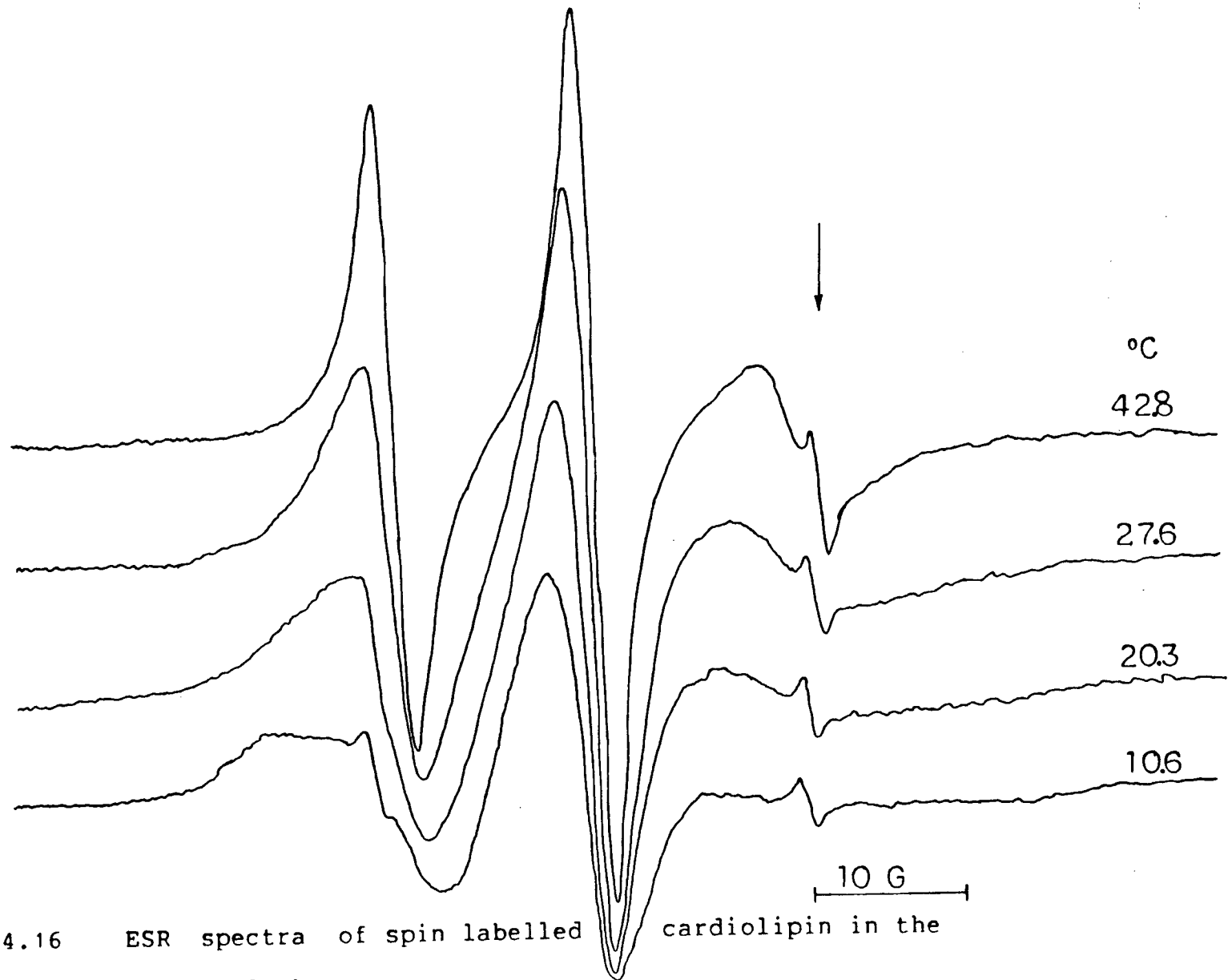

Figure 4.16 ESR spectra of spin labelled cardiolipin in the hexagonal phase.

recorded before for the lamellar phase. The ESR spectra obtained indicate that the motion monitored by the SLCL to be in the slow motion regime at low temperatures and in an intermediate motion regime at higher temperatures. The ESR spectra also showed a very small amount of free nitroxide spin probe was present in the sample (indicated by an arrow) possibly from the degradation of the SLCL or from unreacted spin label.

4.10 SLCL in Hexagonal Phase with Excess of Ca^{2+}.

No lineshape change for the SLCL was observed when Ca^{2+} concentration was kept constant and the concentration of cardiolipin varied. This result is in agreement with the result obtained with the 5-doxyl-stearic acid spin probe.

When the concentration of cardiolipin was kept constant and the concentration of Ca^{2+} varied the lineshape changed drastically. In figure 4.17 ESR spectra of SLCL monitoring the hexagonal phase of cardiolipin at various Ca^{2+} concentrations at about 20°C are shown. The change in lineshape indicates less motion in the system as the Ca^{2+} concentration is increased. A plot of the low temperature result at various Ca^{2+} concentrations is shown in figure 4.18 for the slow motion lineshape where T_{11}' can be measured. Again a small amount of free nitroxide spin probe is present.

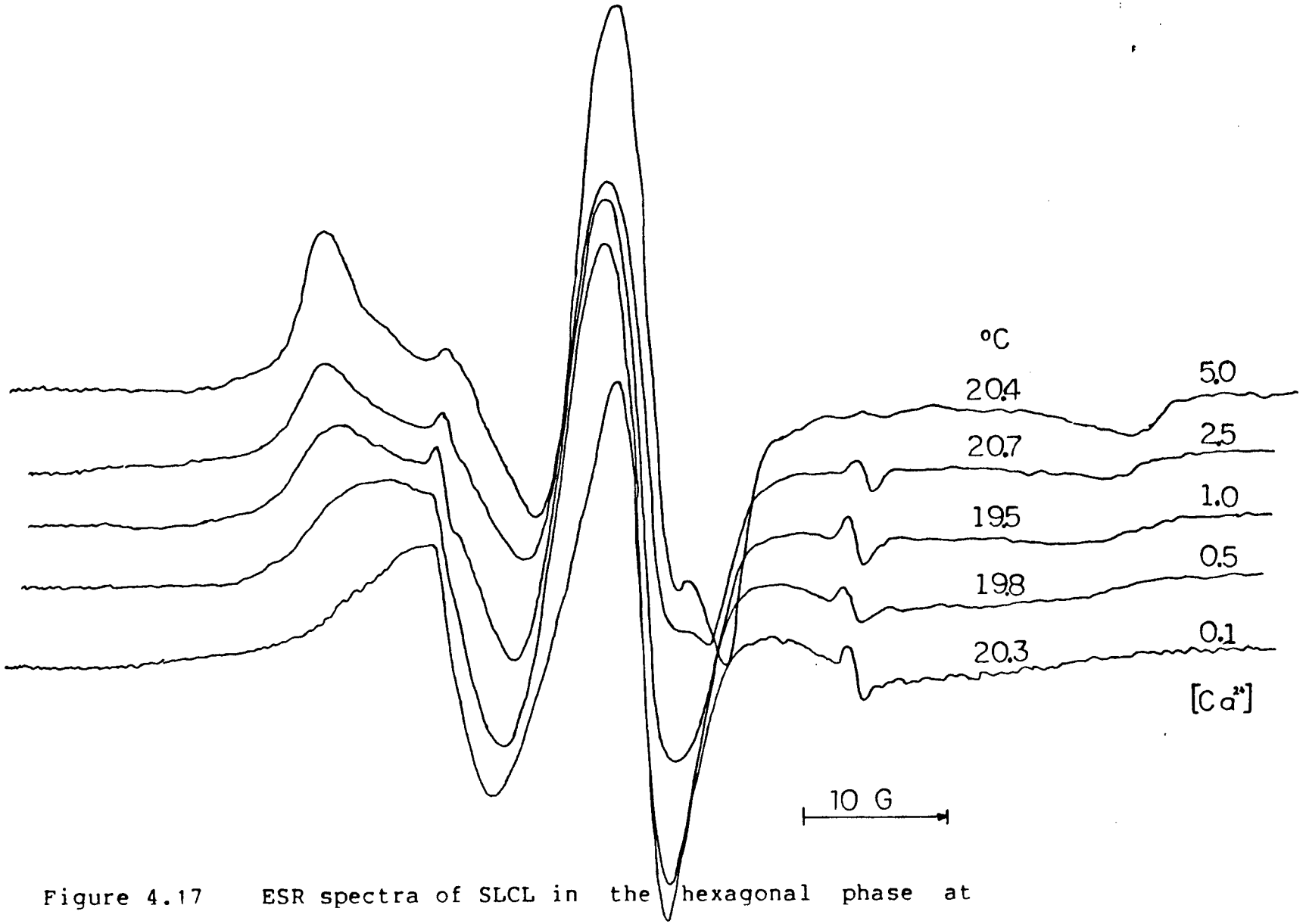

Figure 4.17 ESR spectra of SLCL in the hexagonal phase at various Ca^{2+} concentrations.

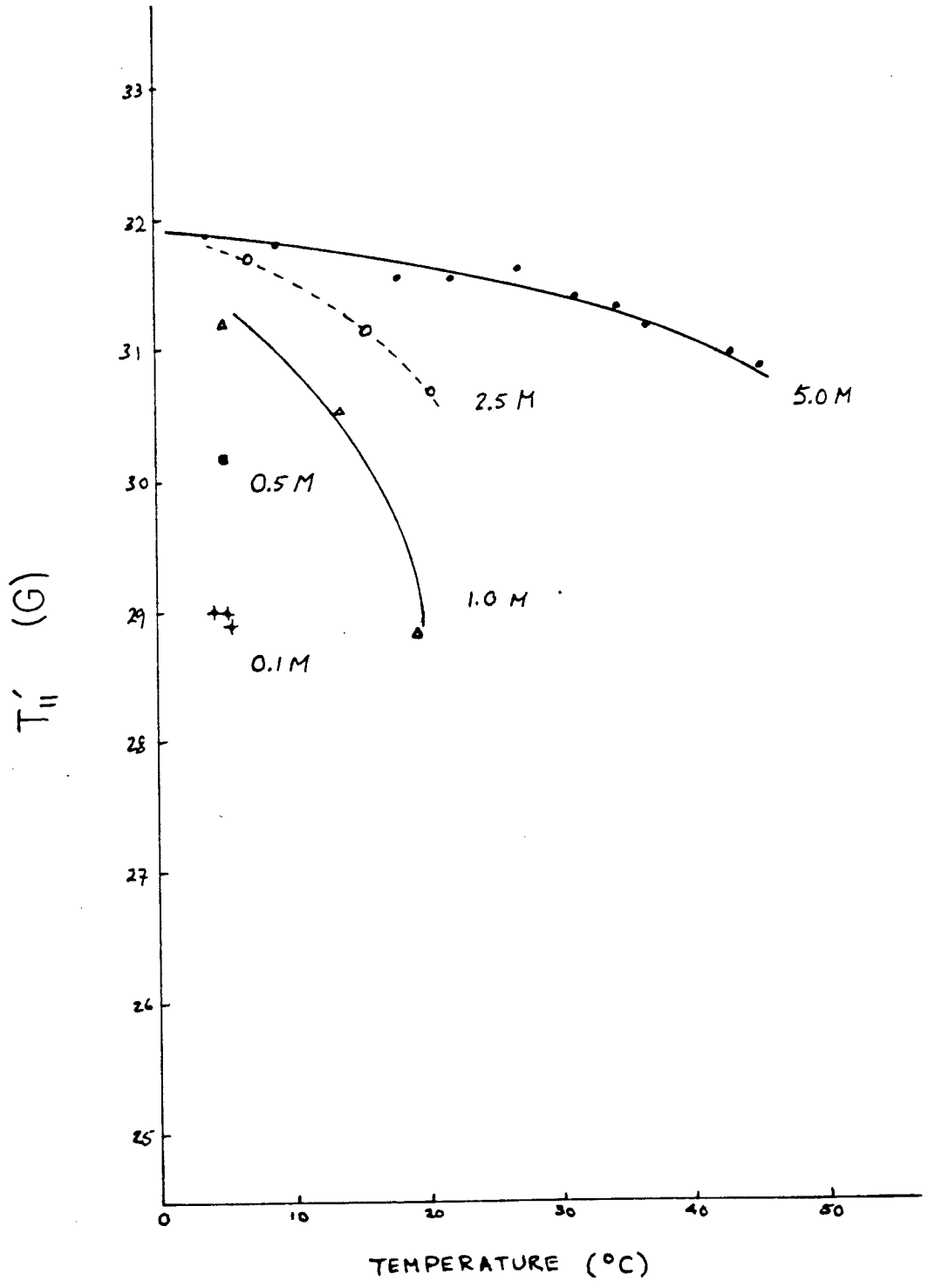

Figure 4.18 T'_{11} vs temperature for SLCL in various Ca^{2+} concentrations.

4.11 SLCL in Mixed Phases.

SLCL in the mixed phase was attempted. An ESR spectrum of SLCL in the ordered lamellar phase at about 20°C is shown in figure 4.19. The spectrum clearly consists of two overlapped spectra, one from the probe in the lamellar phase and the other in a more restricted region where the motion is slower. Thus, as in the case of 5-doxyl stearic acid probe, we have evidence of two phases (or structures) in the presence of Ca^{2+} at less than 1:1 mole ratio. Unfortunately it was not possible to quantitate the mixture of phases due to variable calcium concentration introduced in the preparation of the SLCL.

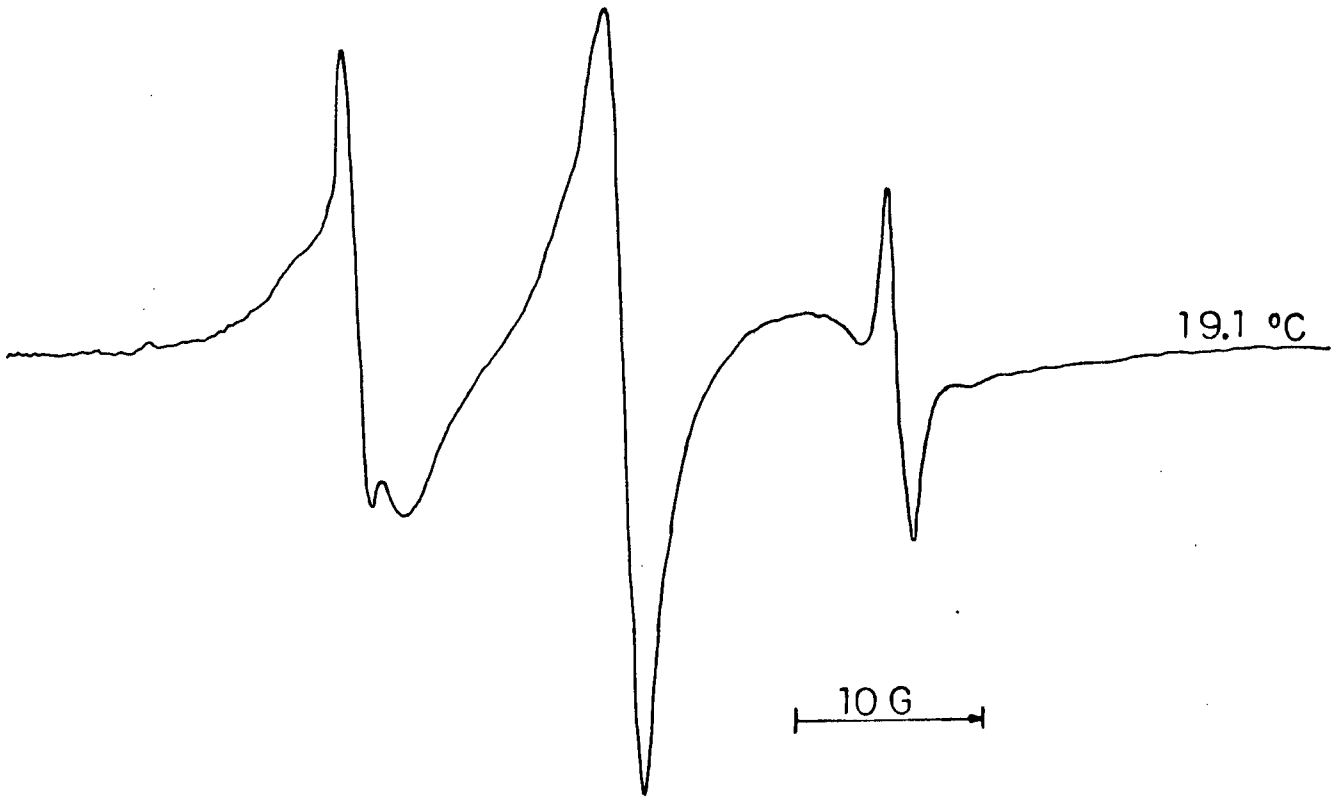

Figure 4.19 ESR spectrum of SLCL in mixed phases.

CHAPTER 5

DISCUSSION

5.1 ESR Studies of The Lamellar and Hexagonal Phase of Cardiolipin.

ESR spectra from 5-doxyl-stearic acid spin probe incorporated in the cardiolipin lamellar phase provides information about the mobility of the spin probe or indirectly the fluidity of the lamellar phase. The ESR data showed that T_{11}' for the spin probe is linearly dependent on temperature over the temperature ranges 4-37°C and 37-60°C and with a discontinuity at 37°C. The linear dependence of T_{11}' of the spin probe on temperature can be interpreted as due to an increase in the fluidity (order and mobility) of the lipid as temperature is increased. The discontinuity can be interpreted as the thermotropic phase transition of the disodium cardiolipin.

The phase transition of aqueous dispersions of cardiolipins has been studied by differential scanning calorimetry [28]. It was found that the phase transition temperature of 16:0 cardiolipin is 39.5°C and the temperature increases by 15°C for each ethyl residue addition. Thus, since cardiolipin from beef heart is mainly linoleic (18:1) acyl chains, we might expect the transition temperature to be 55°C, this phase transition temperature is approximately 18°C higher than from our result. The lower transition temperature is almost certainly due to the presence of the double bond [14].

The gel-to-liquid crystalline thermotropic phase transition

is not of the cardiolipin itself, since no thermotropic transition was detected for the dry lipid sample [28]. This transition is a characteristic of the bilayer organization assumed by the hydrated cardiolipin. The abrupt change of the fluidity of the lamellar phase is attributed to a change in the packing of the lipid in the bilayer [14,28].

Results from the spin probe incorporated in the cardiolipin hexagonal phase showed a non-linear relationship of T_{II}' with respect to temperature and no discontinuity over the range of 3-55°C. In the presence of Ca^{2+} the transition observed in the lamellar phase does not occur [14]. This observation is expected since the gel-to-liquid crystalline transition for calcium cardiolipin is expected to be at 90°C [28]. The nonlinear dependence of the spin probe motion to temperature can be viewed as a combination of the effect of more fluid lipid as temperature increased, the decreasing size of the water channel and overall compacting of the hexagonal phase with temperature [11]. So as the temperature is increased the added motion of the probe is partially cancelled out by the more ordered lipid until the temperature effect dominates the lipid structure effect.

The results from our study of the cardiolipin lamellar and hexagonal phases with the spin labelled cardiolipin confirm the results using the 5-doxyl-stearic acid spin probe. The spectra from the SLCL in the lamellar phase showed the spin label to be in the fast motional regime. This is to be expected since the spin label is monitoring the aqueous phase above the bilayer. So no discontinuity is expected as it is not monitoring the bilayer. This is an indirect way of indicating that the

nitroxide moiety is in fact located on the head group. The ratio of $\tau_c / \tau_B > 1$ from the result indicate the preferred axis for rotation is the Y axis [25]. A model of the position of the nitroxide moiety in the bilayer and the preferred axis of rotation is shown in figure 5.1.

A further indication of the spin label on the head group is that when Ca^{2+} is introduced to the system, the ESR spectra changed drastically from indicating rapid motion to that reflecting a much more immobile probe. This indicates the aqueous phase available to the spin label in the hexagaonal phase is very restrictive. When the spin label is in the hexagonal phase it is in a cylindrical aqueous channels of 15 Å diameter, thus its motion is more restricted than the lamellar phase.

As indicated in chapter 4 our results for the study of the lamellar phase and the hexagonal phase are in agreement with the results of Hegner et al [14] and not with the results of Hsia et al [15]. The spin probe used for our experiments was the same one used by Hegner et al but slightly different from the one used by Hsia et al. The difference in the spin probes are in the length of the hydrocarbon chain. The Hsia group used the 5-doxyl-palmitic acid probe which is two carbon length shorter than the 5-doxyl-stearic acid probe. This difference does not create a significant problem since both of the spin moieties are on the fifth carbons and are monitoring the environment around this region.

The slight difference in the spin probes used does not account for the discrepences in the results. To compare the

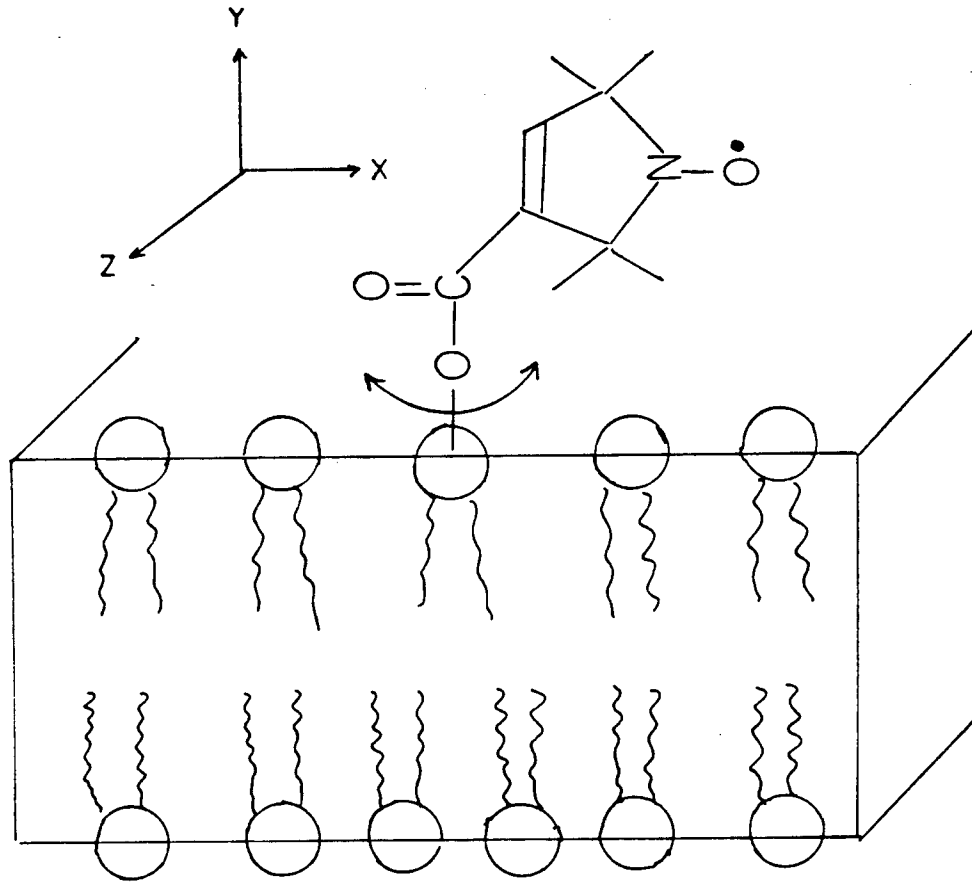

Figure 5.1 SLCL in the lamellar phase indicating its preferred motion.

results we have assumed that room temperature referred to in the Hsia paper to be 25°C. At 25°C our results and that of Hegner's indicated T_{11}' for lamellar phase to be 23.0 G and for the hexagonal phase 28.5 G while Hsia's are 25.3 G and 25.2 G respectively.

A possible explanation for the difference can be found from our results on the Ca^{2+} titration experiment. The results indicate that if a small amount of Ca^{2+} is present, as little as 9 mole percent , the T_{11}' is increased from 23.0 to 25.5 G at 25°C. As mentioned in section 4.3, a similar splitting is also observed when EDTA is not used in forming the lamellar dispersion i.e. Ca^{2+} impurity (found to be up to 3 mole % of Ca^{2+} [11]) in the cardiolipin causes an increase in the splitting (T_{11}').

To explain the apparent decrease in T_{11}' for the hexagonal phase, we have found that the cardiolipin will precipitate out at approximately 38 mole % of Ca^{2+} i.e. 0.6 to 1 mole ratio Ca^{2+} to cardiolipin. At this concentration the value of T_{11}' is 26.0 G which is similar to that observed by Hsia et al. At a mole ratio of 1:1 the splitting is 28.5 G. Thus a possible explanation of the Hsia result for the hexagonal phase is that the Ca^{2+} to cardiolipin ratio was less than one.

5.2 ESR Studies of cardiolipin with varing amounts and concentration of Ca^{2+}.

Prior to disscussing our results it is useful to review the current view of the formation of the hexagonal phase. X-ray studies have shown that in the absence of divalent cation such

as Ca^{2+}, cardiolipin assumes the bilayer structure as in figure 1.4 [11]. The introduction of equimolar of Ca^{2+} causes the cardiolipin to form the hexagonal phase (figure 1.4). These findings are supported by ^{31}P NMR [10,29] and freeze-fracture [12,30] experiments. These techniques were also used to follow the cardiolipin as it proceeds from the bilayer to the hexagonal arrangement [29,31]. These studies show that cardiolipin forms the hexagonal structure via an intermediary phase.

The observation of an intermediary phase by ^{31}P NMR was characterized by isotropic motional averaged signal. The addition of Ca^{2+} to the lamellar phase results in the formation of lipid structures visualized as particles or pits on the freeze-fracture micrographs. These pits were interpreted as inverted lipid (see figure 5.2) structures sandwiched between the the two monolayers of the lipid bilayer [32-35]. The presence of these Ca^{2+}-induced 'lipidic particles' is the starting point of the formation of the tubes of the hexagonal phase.

The model to decribe the formation of the hexagonal phase is as shown in in figure 5.2. The lamellar phase is formed by dispersing the cardiolipin in the absence of divalent cation with buffered Na^{+} solution. As Ca^{2+} is added to the system, it is distributed randomly over the surface of the lamellar phase. When this happens some of the cardiolipin will be converted to the calcium salt form and assumes a cone-shape. To accommadate this new cone-shape in the midst of cylindrical shaped of unchelated cardiolipin the bilayer will be altered to form depressions in the structure. As more Ca^{2+} are added more pits

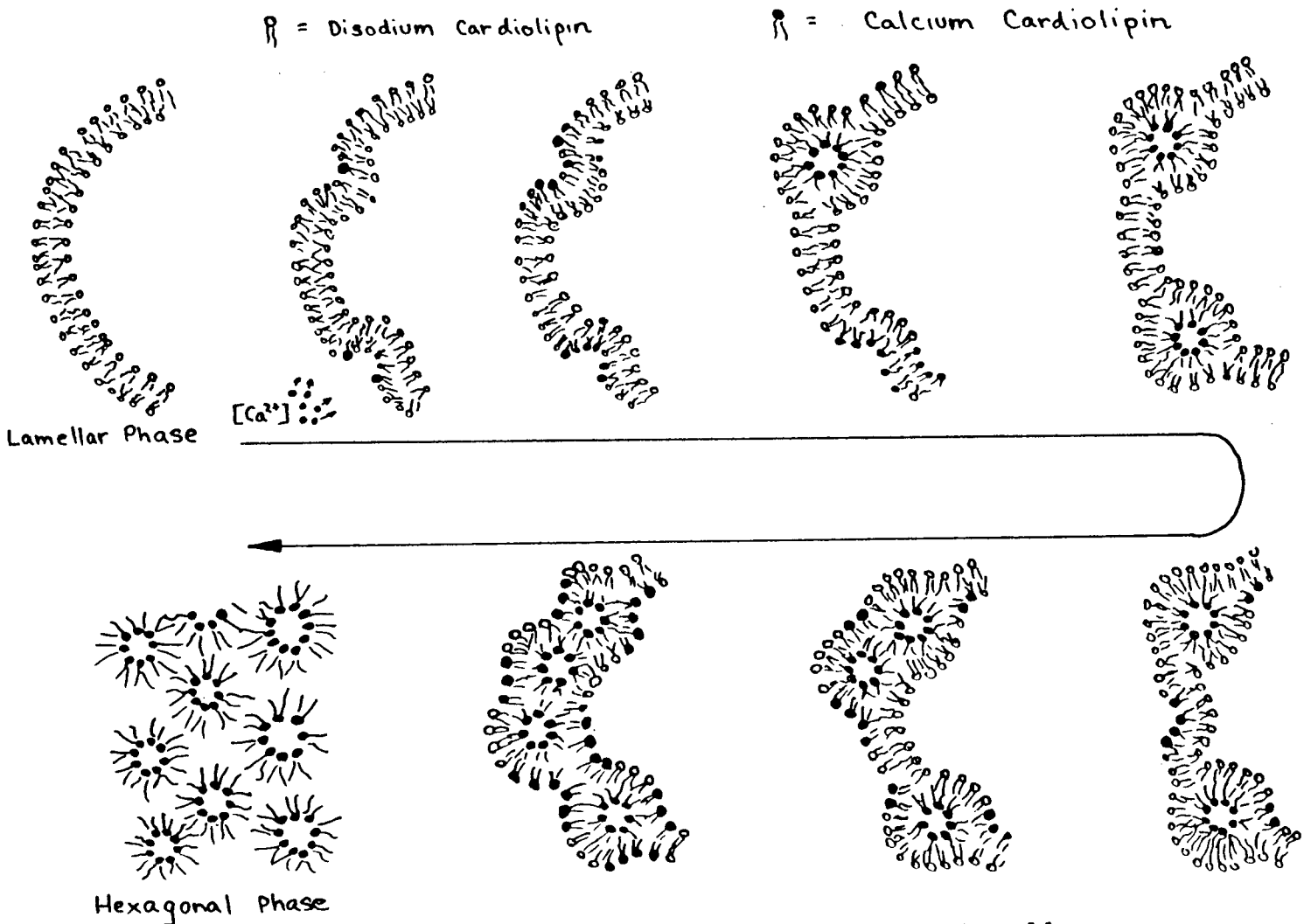

Figure 5.2 Model for the phase transition from the lamellar phase to the hexagonal phase with the addition of Ca^{2+}.

are formed and some will start to go into the inverted micelle confirguration. More inverted micelles are formed as more Ca^{2+} is added. When further Ca^{2+} is added to the system inverted micelles are formed ontop of inverted micelles. The inverted micelles may fuse together during this process but still stay in the lamellar dispersion. At approximately 38 mole % of Ca^{2+} added these fused inverted micelles form tubes of inverted micelle and start to precipitate out of solution. When 1:1 cardiolipin to Ca^{2+} mole ratio is reached all the lipid precipitates out as hexagonal phase. We shall now discuss this model in the light of our ESR studies.

The effect of excess Ca^{2+} on the cardiolipin hexagonal phase was studied in two sets of experiments. In one, the Ca^{2+} concentration was kept constant and the other two component in the cardiolipin-Ca^{2+}-water system were varied. In this experiment the Ca^{2+}/water ratio was kept constant while cardiolipin/Ca^{2+} and cardiolipin/water ratio were decreased. The cardiolipin/Ca^{2+} ratio was varied from 1:1 up to 1:15 with no apparent change in the ESR spectrum of the 5-doxyl-stearic acid probe. This showed that when the mole ratio of cardiolipin to Ca^{2+} is 1:1, the excess amount of Ca^{2+} will not alter the lipid packing of the hexagonal phase.

The second set of experiments, the cardiolipin/water ratio was kept constant while the Ca^{2+}/water ratio was increased and cardiolipin/Ca^{2+} ratio was decreased. The Ca^{2+}/water ratio was varied from 0.1 to 5.0 with drastic change in the ESR spectra of the spin probe. The T'_{11} change in the ESR spectra at room temperature went from 29 G to 32 G indicating an increase in

order and less motion in the lipid structure. This shows that the lipid in the hexagonal structure is being compacted together as the Ca^{2+} concentration is increased. This result is supported by X-ray data [11] that the polar to polar head distance was decreased with increased Ca^{2+} concentration. This can be viewed as the lipid becoming more and more dehydrated as the Ca^{2+} concentration is increased.

The 5-doxyl-stearic acid results were further supported by the results from the SLCL studies. When the Ca^{2+} concentration was increased from 0.1M to 5.0M the ESR spectra of SLCL indicated less motion (see figure 4.17). Since the nitroxide moiety is on the head group, this indicates that the water channels are restricting the motion of the probe as the Ca^{2+} concentration is increased. Again if the hexagonal phase is becoming dehydrated then the water channels will obviously get smaller.

To investigate the phase transition of cardiolipin from lamellar phase to hexagonal phase, a Ca^{2+} titration experiment was performed. In this experiment the Ca^{2+} present in the system was increased systematically in steps until a 1:1 mole ratio of cardiolipin to Ca^{2+} was achieved. Variable temperature studies of T' parameter were carried out at each Ca^{2+} addition to monitor the progress of the lipid transition. The results indicate the lamellar phase becomes more ordered when very small amounts of Ca^{2+} is present. The amount of Ca^{2+} can be as little as the inherent impurity present in the lipid. Our results indicate this ordered lamellar stage presists up to about 38 mole % of Ca^{2+} when the lipid starts to precipitate out.

The ordered lamellar phase was induced by the introduction of a small amount of Ca^{2+} into the system. The cylindrical shape of cardiolipin is typical of the disodium cardiolipin and a cone-shape is that of the calcium cardiolipin. Thus when Ca^{2+} was introduced into the lamellar phase the calcium cardiolipin formed will assumme a cone-shape and thus disturb the lamellar bilayer packing. To accommadate the cone-shape the lipids around it will try to conform to this new shape and doing so form dips and pits in the bilayer structure as illustrated in figure 5.2. The packing of the fatty acyl chains will thus change and hence we might expect changes in the observed spectrum of a spin probe incorporated into such structure.

The ESR spectra of the spin probe in a cardiolipin dispersion containing 9-29 mole % of Ca^{2+} showed spectra unlike that from the lamellar or the hexagonal phase. From this we can say that the 5-doxyl-stearic acid spin probe is monitoring a phase that is different from that of the lamellar or the hexagonal phase. The ESR spectra indicated a more ordered environment than the lamellar phase. We suggest that these structures are multilamellar structures with pits and dips caused by the Ca^{2+} leading to a higher order parameter for the spin probe.

The order parameters S for the 5-doxyl stearic acid spin probe in the different phases were calculated using equation 2.9. The order parameters S are listed in table 5.1 and plotted against Ca^{2+} concentration in figure 5.3. The results show that when Ca^{2+} is added to the system the order parameter S is increased significantly from the lamellar phase. The order

Table 5.1

mole % of Ca^{2+}	Order Parmeter S	Temperature (°C)
0.0 (Lamellar Phase)	0.559 0.434 0.351	20.5 32.4 39.0
9	0.598 0.533 0.522	19.8 33.4 39.2
17	0.610 0.538 0.519	19.4 33.6 40.1
29	0.609 0.527 0.511	19.3 32.8 39.7
38	0.625 0.577 0.517	19.4 29.5 39.6
41	0.704 0.602 0.552	17.8 27.9 36.7
47	0.715 0.646 0.574	18.8 28.4 38.8
50 (Hexagonal Phase)	0.771 0.696 0.588	18.1 28.3 39.9

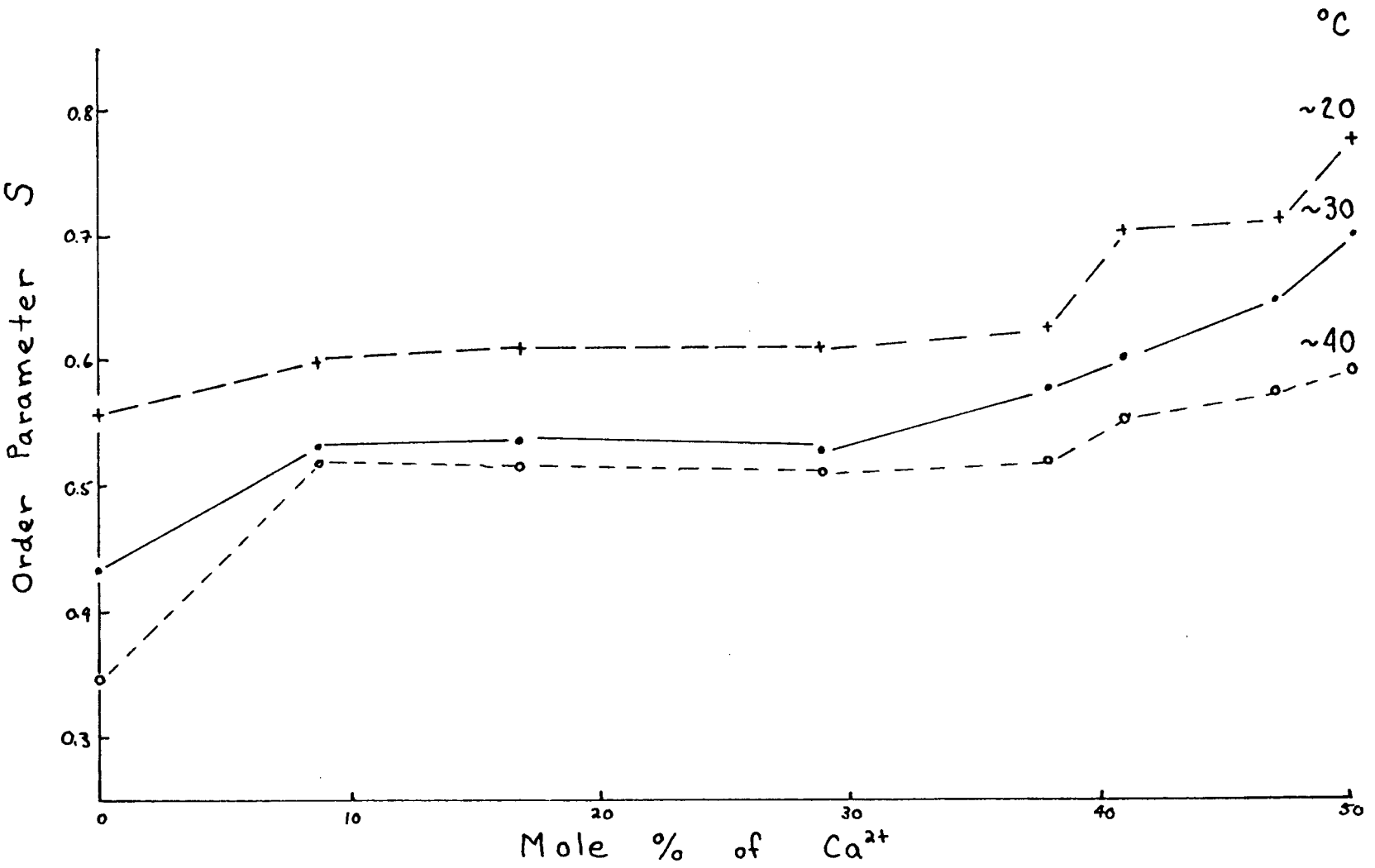

Figure 5.3 Order parameter S vs mole % of Ca^{2+} for 5-doxyl stearic acid spin probe in the cardiolipin at various temperature

parameter stays constant up to about 38 mole percent of Ca^{2+} added and then to higher order in the hexagonal phase.

When the temperature is increased in the presence of 9-29 mole % of Ca^{2+} to 40°C two spectra are observed. One spectrum corresponds to the lamellar phase and the other one is distinct from either the lamellar or the hexagonal phases. This can be explained by assuming that temperature induces the formation of inverted micelles. Thus when there is a small amount of Ca^{2+} present and the temperature of the system is raised, the lipid structure changes as shown in figure 5.4. The calcium salt form of cardiolipin moves to small pools of calcium cardiolipin to form inverted micelles. This lateral phase separation of the calcium cardiolipin may be expected since the inverted micelle is more stable at higher temperatures [11,32]. When this happens we have pockets of inverted micelles and pockets of lamellar structure within the same system. The order and motion will be different in both leading to two distinct spectra.

The above model is supported by X-ray studies [11] performed on Ba^{2+} cardiolipin which behaves the same way. At low temperatures the Ba^{2+} cardiolipin exists as both the lamellar and hexagonal phases and when the temperature is raised only the hexagonal phase is present. The inverted micelle is therefore the more stable structure as the temperature is raised. Further evidence to support this theory is the result of the SLCL study in the presence of Ca^{2+}. Our result indicates that in the presence of Ca^{2+} the spin probe is monitoring two phases (figure 4.19) in which the probe undergoes quite different motion, as is to be expected, if inverted micelles are present in the lamellar

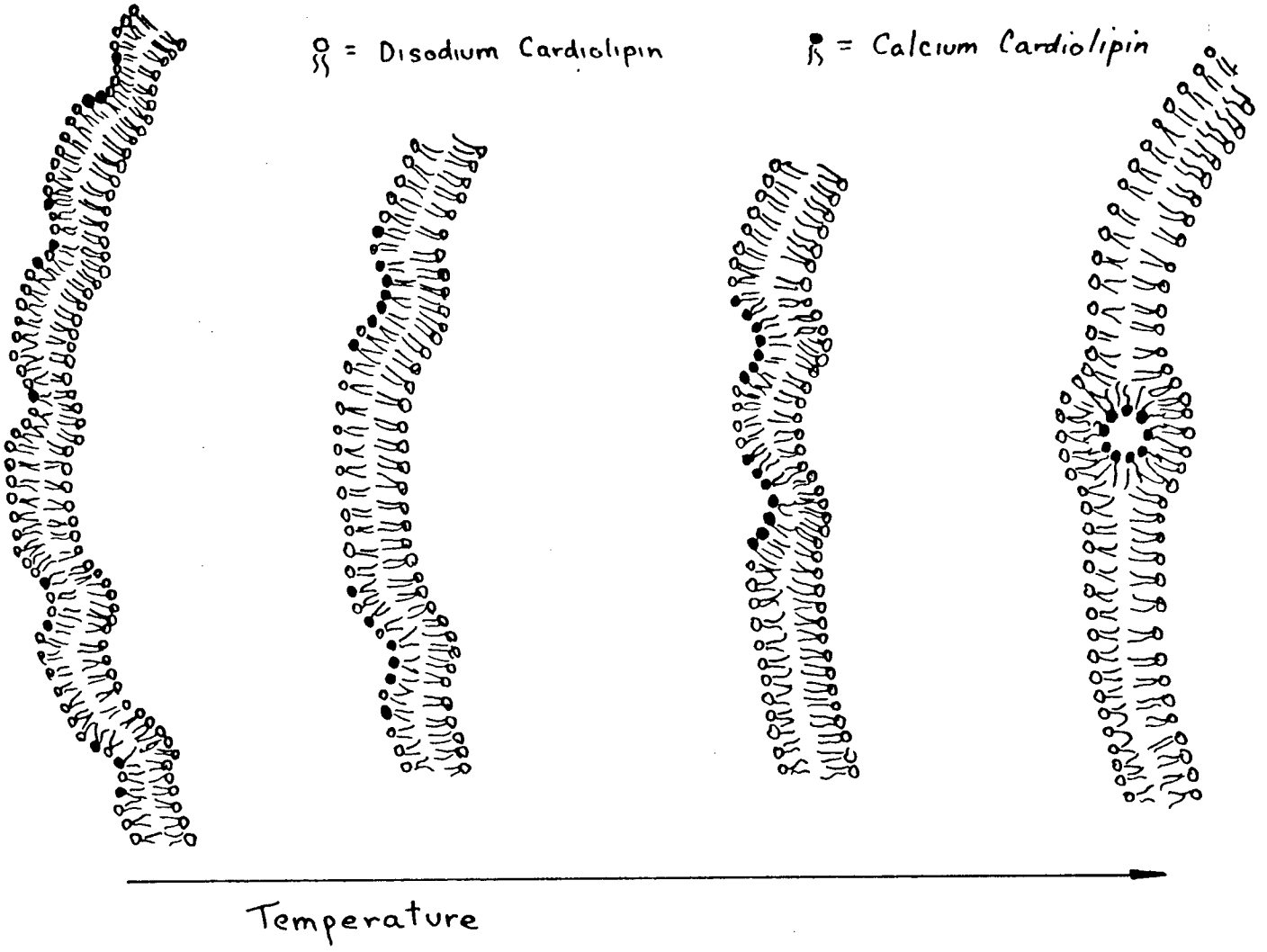

Figure 5.4 Model for the lateral phase separation of Ca^{2+}-cardiolipin.

phase.

5.3 Conclusions.

The work described here has provided valuable additional information on the phase structure of cardiolipin and the interaction between cardiolipin and Ca^{2+}. It has provided supportive evidence for the formation of lipidic particles i.e. inverted micelles [34]. The spin probe study has indicated that at Ca^{2+}/cardiolipin mole ratio of less than 0.6:1 there is an initial lamellar-like structure with pits and dips on its surface [31]. This lamellar-like structure has a fluidity (order and motion) different from that of lamellar or hexagonal cardiolipin and that this structure can be induced to go over to a lamellar structure with inverted micelles imbedded in it. It is at this point two distinct spectra are observed.

The studies with SLCL have shown that this is potentially a very useful tool in the study of the various structures and phases of cardiolipin. It is extremely sensitive to the changes in motion brought about by the formation of inverted micelles and hexagonal phase. Consequently, although not attempted in this work, we feel that the SLCL can be use fully employed in the study of the function of cardiolipin in the lipoprotein erythrocyte acetylcholinesterase [9].

The further studies that might be contemplated at this point are the use of spin probes and spin labels in the study of cardiolipin in the presence of other cations (Ba^{2+}, Mg^{2+}). Cardiolipin in the presence of these cations will form lamellar and or hexagonal phases depending on temperature [11]. These

studies will give additional evidence for the hypothesis of temperature induced phase separation. Other evidence may be obtained by using a mixture of cardiolipin with other lipids that do not form the hexagonal phase. Mixtures of cardiolipin and phosphatidylcholine will form the mixed phases with the addition of Ca^{2+} to the system [32-35]. Furthermore the SLCL could be used in clinical studies in the serological testing of syphilis.

BIBLIOGRAPHY

1. M. C. Pangborn, J. Biol. Chem., 143, 247-256 (1942)

2. Von A. Wassermann, A. Neissen, C. Bruck, Deut. Med. Wach., 32, 745-746 (1906)

3. C. H. Browning, J. Cruickshank, W. Gilmour, J. Pathology and Bacteriology, 15, 361-362 (1911)

4. M. G. MacFarlane, Advances in Lipid Research, 2, 91-125, (1964)

5. P. V. Ioannou, B. T. Golding, Prog. Lipid Res., 17, 279-318 (1979)

6. F. Ramirez, P. V. Ioannou, J. F. Marecek, G. H. Dodd, B. T. Golding, Tetrahedron, 33, 599-608 (1977)

7. M. C. Pangborn, J. Biol. Chem., 168, 351-361 (1947)

8. A. J. Slotboom, P. P. M. Bonsen, Chem. Phys. Lipids, 5, 301-398 (1970)

9. G. Beauregard, B. D. Roufogalis, Biochim. Biophys. Acta, 5, 57, 102-111 (1979)

10. P. R. Cullis, B. De Kruijff, Biochim. Biophys. Acta, 559, 399-420 (1979)

11. R. P. Rand, S. Sengupta, Biochim. Biophys. Acta, 255, 484-492 (1972)

12. D. W. Deamer, R. Leonard, A. Tardieu, D. Branton, Biochim. Biophys. Acta, 219, 47-60 (1970)

13. P. R. Cullis, B. De Kruijff, Biochim. Biophys. Acta, 507, 207-218 (1978)

14. D. Hegner, U. Schummer, G. H. Schnepel, Biochim. Biophys. Acta, 307, 452-458 (1973)

15. J. M. Boggs, J. C. Hsia, Proc. Nat. Acad. Sci. U.S.A., 70, 1406-1409 (1973)

16. M. B. Cable, J. Jacobus, G. L. Powell, Proc. Nat. Acad. Sci. U.S.A., 75, 1227-12431 (1978)

17. C. Landriscina, F. M. Megli, E. Quagliariello, Analytical Biochemistry, 76, 292-299 (1976)

18. J. F. W. Keana, A. R. Ertle, Chem. And Phys. Of Lipids, 17, 402-406 (1976)

19. L. J. Berliner (Ed), Spin Labelling, Theory and Application, Academic Press (1976)

20. J. R. Bolton, D. Berg, H. Swartz, Biological Applications of Electron Spin Resonance, Wiley-Interscience (1972)

21. P. F. Knowles, D. Marsh, H. W. E. Rattle, Magnetic Resonance of Biomolecules, Wiley-Interscience (1976)

22. S. Schreier, C. F. Polnaszek, I. C. P. Smith, Biochim. Biophys. Acta, 515, 395-436 (1978)

23. G. I. Likhtensheein, Spin Labeling Methods in Molecular Biology, Wiley-Interscience (1976) P. S. Shelnitz (Translator)

24. J. F. W. Keana, Chemical Reviews, 78(1), 37-64 (1978)

25. C. F. Polnaszek, S. Schreier, K. W. Butler, C. P. Smith, J. Of The American Chem. Society, 100, 8223-8232,(1978)

26. E. G. Rozantsev, Free Nitroxyl Radicals, Plenum Press (1970) B. J. Hazzard (Translator)

27. H. Okuyama, S. Nojima, J. Of Biochemistry, 57, 529-538 (1965)

28. S. Rainier, M. K. Jain, F. Ramirez, P. V. Ioannou, J. F. Marecek, R. Wagner, Biochim. Biophys. Acta, 558, 187-198 (1979)

29. P. R. Cullis, A. J. Verkleij, P. H. J. Th. Ververgaert, Biochim. Biophys. Acta, 513, 11-20 (1978)

30. P. Arslan, M. Beltrame, U. Muscatello, Micron, 11, 115-125 (1980)

31. W. J. Vail, J. G. Stollery, Biochim. Biophys. Acta, 551, 74-84 (1979)

32. B. De. Kruijff, A. J. Verkley, C. J. A. Van. Echteld, W. J. Gerritsen, C. Mombers, P. C. Noordam, J. De. Gier, Biochim. Biophys. Acta, 555, 200-209 (1979)

33. W. J. Gerritsen, B. De Kruijff, A. J. Verkleij, J. De Gier, L. L. M. Van Deenen, Biochim. Biophys. Acta, 598, 554-560 (1980)

34. A. J. Verkleij, C. Mombers, W. J. Gerritsen, L. Leunissen-Bijvelt, P. R. Cullis, Biochim. Biophys. Acta, 555, 358-361 (1976)

35. J. G. Mandersloot, W. J. Gerritsen, J. Leunissen-Bijvelt, C. J. A. Van Echteld, P. C. Noordam, J. De Gier, Biochim. Biophys. Acta, 640, 106-113 (1981)

36. J. C. Tait, Ph. D. Thesis, University of British Columbia (1974)